International Journal of Biological Macromolecules 189 (2021) 744–757

Contents lists available at ScienceDirect

International Journal of Biological Macromolecules

journal homepage: www.elsevier.com/locate/ijbiomac

Development of mushroom polysaccharide and probiotics based solid self-nanoemulsifying drug delivery system loaded with curcumin and quercetin to improve their dissolution rate and permeability: State of the art

Rubiya Khursheed [a], Sachin Kumar Singh [a,*], Sheetu Wadhwa [a], Monica Gulati [a], Bhupinder Kapoor [a], Subheet Kumar Jain [b], Kuppusamy Gowthamarajan [c,d], Flavia Zacconi [e,f], Dinesh Kumar Chellappan [g], Gaurav Gupta [h], Niraj Kumar Jha [i], Piyush Kumar Gupta [j], Kamal Dua [k,l]

[a] School of Pharmaceutical Sciences, Lovely Professional University, Phagwara, Punjab 144411, India
[b] Department of Pharmaceutical Sciences, Guru Nanak Dev University, Amritsar, India
[c] Department of Pharmaceutics, JSS College of Pharmacy, JSS Academy of Higher Education & Research, Ooty, Nilgiris, Tamil Nadu, India
[d] Centre of Excellence in Nanoscience & Technology, JSS College of Pharmacy, JSS Academy of Higher Education & Research, Ooty, Nilgiris, Tamil Nadu, India
[e] Departamento de Química Orgánica, Facultad de Química y de Farmacia, Pontificia Universidad Católica de Chile, Av. Vicuña Mackenna 4860, Macul, Santiago 7820436, Chile
[f] Institute for Biological and Medical Engineering, Schools of Engineering, Medicine and Biological Sciences, Pontificia Universidad Católica de Chile, Av. Vicuña Mackenna 4860, Macul, Santiago 7820436, Chile
[g] Department of Life Sciences, School of Pharmacy, International Medical University, Bukit Jalil, 57000 Kuala Lumpur, Malaysia
[h] School of Pharmacy, Suresh Gyan Vihar University, Mahal Road, Jagatpura, Jaipur, India
[i] Department of Biotechnology, School of Engineering & Technology (SET), Sharda University, Greater Noida 201310, India
[j] Department of Life Sciences, School of Basic Sciences and Research, Sharda University, Knowledge Park III, Greater Noida, Uttar Pradesh 201310, India
[k] Discipline of Pharmacy, Graduate School of Health, University of Technology Sydney, Ultimo, NSW 2007, Australia
[l] Faculty of Health, Australian Research Centre in Complementary and Integrative Medicine, University of Technology Sydney, Ultimo, NSW 2007, Australia

ARTICLE INFO

Keywords:
Mushroom polysaccharides
Probiotic
Spray drying

ABSTRACT

The role of mushroom polysaccharides and probiotics as pharmaceutical excipients for development of nanocarriers has never been explored. In the present study an attempt has been made to explore *Ganoderma lucidum* extract powder (GLEP) containing polysaccharides and probiotics to convert liquid self nanoemulsifying drug delivery system (SNEDDS) into solid free flowing powder. Two lipophilic drugs, curcumin and quercetin were used in this study due to their dissolution rate limited oral bioavailability and poor permeability. These were loaded into liquid SNEDDS by dissolving them into isotropic mixture of Labrafill M1944CS, Capmul MCM, Tween-80 and Transcutol P. The liquid SNEDDS were solidified using probiotics and mushroom polysaccharides as carriers and Aerosil-200 as coating agent. The solidification was carried out using spray drying process. The process and formulation variables for spray drying process of liquid SNEDDS were optimized using Box Behnken Design to attain required powder properties. The release of both drugs from the optimized spray dried (SD) formulation was found to be more than 90%, whereas, it was less than 20% for unprocessed drugs. The results of DSC, PXRD and SEM, showed that the developed L-SNEDDS preconcentrate was successfully loaded onto the porous surface of probiotics, mushroom polysaccharides and Aerosil-200.

1. Introduction

Numerous novel active molecules having great pharmacological activity are coming up due to progress in current drug discovery programs. Despite such a vast therapeutic potential these new molecules are not gaining much attention in the clinical field due to their inherent

* Corresponding author at: School of Pharmaceutical Sciences, Lovely Professional University, Phagwara 144411, Punjab, India.
E-mail address: sachin.16030@lpu.co.in (S.K. Singh).

https://doi.org/10.1016/j.ijbiomac.2021.08.170
Received 9 June 2021; Received in revised form 18 August 2021; Accepted 22 August 2021
Available online 28 August 2021

challenge of low aqueous solubility resulting in poor bioavailability. Various attempts have been made to enhance the solubility of these drugs. Some of the attempts include solid dispersion [1], micelles [2], solid lipid nanoparticles [3], nanoliposomes [4], niosomes [5], nanorod [6], nanostructured lipid carriers [7], etc. Recently self nano emulsifying drug delivery system (SNEDDS) has gained much attention in overcoming the above mentioned challenges. Compared to other dosage forms SNEDDS offer the advantage of fast onset action, ease of formulation, and scale up and dose reduction. Moreover, SNEDDS as drug delivery system offer additional advantages as they protect the drugs from gastrointestinal degradation and first pass metabolism since the drug gets absorbed through lymphatic system. Despite these advantages liquid SNEDDS (L-SNEDDS) are not much stable due to precipitation, creaming, cracking issues over time [8,9]. The commonly used technique to overcome the problems associated with the stability of L-SNEDDS is their solidification using powders with greater absorbing capacity for liquids. Commonly, the methods used to convert L-SNEDDS into solid SNEDDS (S-SNEDDS) include conventional adsorption onto inert carriers (surface adsorption technique), extrusion-spheronization, melt granulation and spray drying [10–12]. The most widely and economically used method is adsorption of L-SNEDDS on the surface of porous carriers [13–15]. Adsorption method has benefits of increased oil loading capacity, reduced process loss, easy formulation, easy change of the solidified powder formulation into tablets and economical method [14,16]. Spray drying technique can be used at both industrial as well as laboratory scale as it is fast, single-step, unremitting, reproducible, and consequently, scalable without main alterations. A positive bench-to-bedside transformation of a method depends on the accomplishment of two circumstances: cost-effectiveness and scalability. Spray-drying fulfils both the conditions. A notable benefit is that the powders obtained by spray drying have improved micromeritic characteristics and increased drug loading. The solid particles obtained present relatively narrow size distribution at the submicron-to-micron scale [14,17,18]. Hence, the judicious selection of solid carrier and technique to solidify L-SNEDDS is very important [14,17,18]. The commonly used porous carriers include Aerosil-200 (A-200), hydroxy propyl methyl cellulose (HPMC), lactose, poly vinyl alcohol (PVA), magnesium stearate etc. These porous carriers have been extensively reported to solidify emulsions, nanoemulsions, SNEDDS [10,19]. But these carriers suffer from their own challenges such as A-200 leads to poor compressibility when used at higher concentrations and is also reported to cause toxicity when used in higher amount. Further lactose and other carriers are required in higher amount which can lead to increased bulk of the solid dosage form resulting in patient incompliance [9]. Owing to the limitations of the above mentioned porous carriers a novel approach has been adopted using natural resources [Probiotics (PBs) and mushroom powder containing polysaccharides].

The present study deciphers impact of PBs and mushroom polysaccharide as solid carriers for drying of L-SNEDDS. PBs and mushroom polysaccharides are well reported for their anti-oxidant and anti-inflammatory effects. These are used for the management of diabetes [20], oxidative stress [21], neurodegenerative disorders [22], cardiovascular disorders [23] etc. Thus, besides acting as solid carriers they can provide therapeutic advantages as well.

Curcumin (CUR) and quercetin (QUE) are taken as the model drugs for the present study. These are well known polyphenols and are explored for many therapeutic activities. CUR, commonly known as the golden spice of life has been used from past many years (30–35) for the treatment of arthritis [24], thrombosis [25], neuropathy [26], diabetes [27], cardioprotective effects [28], cancer [29], Parkinson's disorder [30] etc. Similarly, QUE has also been explored from last 25 years for its anticancer activity [31], diabetes [32], hyperlipidemia [32], osteoarthritis [33], anti-arrhythmogenic effects [34] etc. Despite such pharmacological potentials both the drugs are suffering from their inherent challenge of low aqueous solubility and poor permeability resulting in poor bioavailability. To enhance their solubility L-SNEDDS of CUR and QUE were developed. Further the solidification potential of *Ganoderma lucidum* extract powder (GLEP) mushroom polysaccharides and PBs was compared with other solid carriers in terms of micromeritic properties of S-SNEDDS. The formulation was spray dried and the impact of process parameters (inlet air temperature and feed flow rate) and formulation variable (carrier to coating ratio) on micromeritic properties, percentage yield and drug loading was determined using Box Behnken design (BBD). The optimized formulation was characterized by using scanning electron microscopy (SEM), differential scanning calorimetry (DSC), and Powder X-ray diffraction (PXRD). The results were compared with non-spray dried (NSD) product. The final formulation was then subjected to stability studies.

2. Materials and methods

2.1. Materials

CUR was purchased from Molychem, Mumbai, India. QUE dihydrate was purchased from Himedia, Mumbai, India. Propylene glycol (PG), Span 80, Polyethylene glycol (PEG) 200, 400, and 600, microcrystalline cellulose PH102 (MCC PH102), Tween (T) 20 and 80, Aerosil 200 (A-200), magnesium stearate (MS), and lactose were purchased from Central Drug House, New Delhi, India. Sesame oil, olive oil, cotton seed oil, groundnut oil, almond oil, soyabean oil, eucalyptus oil, mustard oil, castor oil were purchased from Global Merchants, Navi Mumbai, India. Labrafil M1944CS (LMCS), Labrafac PG (LPG), Labrasol (LS), Lauroglycol FCC (LFCC), and Transcutol P (TP) were gifted by Gattefosse, Mumbai, India. Capmul MCM (CMCM) was gifted by Abitec Corp., Mumbai, India. GLEP was gifted by Ayush Herbal and Healthcare, Sirmour, India. The GLEP used in the study was containing β-D-glucan (60%, 22,014 Da molecular weight), α-glucan (18.18%), 15.8% total phenolic content (in terms of gallic acid), gallic acid (3.248 μg/g), *Trans*-cinnamic acid (0.164 μg/g), quercetin (1.123 μg/g), kaempferol (1.104 μg/g), hesperetin (6.26 μg/g), naringenin (4.854 μg/g), *p*-coumaric acid (0.125 μg/g), rutin (0.116 μg/g), chlorogenic acid (0.124 μg/g), syringic acid (0.101 μg/g), resveratrol (0.132 μg/g), vanillic acid (0.148 μg/g), *p*-hydroxybenzoic acid (0.169 μg/g), caffeic acid (0.102 μg/g), benzoic acid (0.091 μg/g) and catechin (0.113 μg/g) [9].Triple distilled water (d.w.) was used throughout the study. PB (BIOMIX-1) having composition *Lactobacillus acidophilus* (1.7 billion CFU), *Lactobacillus rhamnosus* (1.7 billion CFU), *Bifidobacterium longum* (1.8 billion CFU), *Bifidobacterium bifidum* (1.8 billion cells), *Saccharomyces boulardii* (0.13 billion CFU) and *Fructooligosaccharides* (100 mg), was gifted by Unique Biotech, Hyderabad, India.

2.2. Methodology

2.2.1. Formulation of L-SNEDDS

Initially, solubility studies were carried out using various oils (LMCS, LPG, LS, CMCM, sesame oil, olive oil, cotton seed oil, groundnut oil, almond oil, soyabean oil, eucalyptus oil, mustard oil, castor oil) and surfactants (TP, T80, T20, PEG200, PEG400, PEG600, LFCC). The results revealed that both the drugs were highly soluble in LMCS, CMCM, T80 and TP. Hence these were selected for formulation of SNEDDS. One L-SNEDDS prototype (1 mL) was prepared by mixing the oils (LMCS and CMCM), surfactant (T80) and co-surfactant (TP) in the ratio of 9.776: 6.228: 38.927: 45.069 v/v using vortex mixer (CM 101 CYCLO MIXER, REMI, New Delhi, India) for 10 min. Subsequently 10 mg of CUR and 10 mg of QUR each were added to this pre-concentrate. This was again followed by vortexing of the mixture for 15 min using vortex mixer. The formulated pre-concentrate was diluted in 500 mL d.w. that was kept on a magnetic stirrer (MS500, REMI, New Delhi, India) at 500 rpm at 37 ± 0.2 °C for 5 min [9].

Table 1
Lf values and micromeritic properties of different carriers used to solidify T80 (n = 3).

S. N	Carrier	Lf (mg)	AOR (θ) (mean ± S.D.)	BD (mean ± S.D.)	TD (mean ± S.D.)	CI (mean ± S.D.)	HR (mean ± S.D.)
1.	Aerosil-200	1.42	20.00 ± 1.33	0.089 ± 0.09	0.104 ± 0.03	14.4 ± 3.11	1.16 ± 0.47
2.	Probiotic	0.14	22.3 ± 1.86	0.49 ± 0.03	0.62 ± 0.59	20.9 ± 2.98	1.26 ± 0.98
3.	GLEP	0.11	34.96 ± 2.11	0.35 ± 0.87	0.43 ± 0.05	18.6 ± 1.05	1.22 ± 0.69
4.	Lactose	0.16	39.6 ± 2.11	0.42 ± 0.16	0.56 ± 0.62	25.0 ± 3.88	1.33 ± 1.03
5.	PVA	0.2	36.1 ± 1.44	0.40 ± 0.11	0.51 ± 0.75	21.5 ± 4.11	1.27 ± 0.99
6.	HPMC	0.25	56.83 ± 3.11	0.22 ± 0.76	0.29 ± 0.09	24.1 ± 1.95	1.31 ± 0.74
7.	MCC PH102	0.2	54.46 ± 1.88	0.29 ± 0.02	0.36 ± 0.08	19.4 ± 3.81	1.24 ± 0.94
8.	PB + GLEP (1:1)	0.41	30.5 ± 2.11	0.50 ± 0.95	0.65 ± 0.42	25 ± 4.71	1.30 ± 0.59
9.	PB + GLEP (1:2)	0.29	39.35 ± 2.78	0.30 ± 0.19	0.52 ± 0.74	52 ± 2.95	2.1 ± `0.53
10.	PB + GLEP (2:1)	0.35	31.2 ± 2.05	0.67 ± 0.07	0.78 ± 0.09	54 ± 5.14	2.5 ± 0.97

2.2.2. Solidification of L-SNEDDS

2.2.2.1. Screening of solid carriers. Initially a number of solid carriers (A-200, HPMC, Lactose monohydrate, PBs alone, PVA, GLEP alone, MCCPH102) were used in order to obtain S-SNEDDS powder with good flow characteristics. The flow characteristics of these blends were compared with the blend containing mixture of GLEP and PBs in 3 different ratios i.e. 1:1, 1:2 and 2:1. In order to formulate S-SNEDDS powder, 10 different mortars were taken and L-SNEDDS preconcentrate (1 mL) was added in each mortar. This was followed by addition of each carrier in individual mortar containing L-SNEDDS preconcentrate and triturated for 5 min to form a uniform mixture. It is important to note that in case where combinations of GLEP and PBs were prepared, an amount equivalent to 350 mg of A-200 was added as coating material in each batch. The carrier addition was continued until a powder with acceptable flow rate was achieved [35]. The loading factor (Lf) which is defined as the fraction of liquid isotropic mixture holding drug [36,37] and calculated using Eq. (1) (Table 1).

$$Lf = \frac{W}{Q} \tag{1}$$

Here, W: amount of liquid isotropic mixture and Q: amount of carrier material

2.2.2.2. Flow properties of S-SNEDDS. All the prepared formulations containing different solid carriers were characterized for flow properties which include angle of repose (AOR), bulk density (BD), tapped density (TD), Carr's compressibility index (CCI) and Hausner's ratio (HR). All the micromeritic properties were determined as specified by Kumar et al., 2018 [38]. Standard funnel method was used to calculate the AOR. A funnel was taken and kept stationary on a smooth working table. Each developed SNEDDS powder formulated using different carriers was transferred separately through this funnel in order to form a cone. The funnel tip was kept near to the mounting cone and gradually raised as the heap grew in order to reduce the influence of dropping particles. The pouring of powder was stopped as the cone attained a fixed measurable height. The height (h) of the pile was calculated from the base of the heap and the diameter was also calculated. The radius (r) was calculated by dividing the diameter by 2. The AOR (θ) was calculated as per Eq. (2) [12].

$$AOR\ (\Theta) = \frac{tan - 1 \times h}{r} \tag{2}$$

The actual powder weight (W) was calculated. A measuring cylinder was taken and joined to an automatic tap density test apparatus (USP type, Electro lab Pvt. Ltd., Mumbai, India). Each formulation was put inside this attached measuring cylinder. Prior to tapping procedure the volume for each powdered formulation was calculated. Subsequently, 200 tappings were given to this cylinder and the attained final volume after tappings was again calculated. The procedure for each powder blend was repeated 3 times. The calculation of BD (ρb), TD (ρt), CCI and HR was carried according to Eqs. (3), (4), (5) and (6) respectively [38].

$$\rho b = \frac{w}{Vb} \tag{3}$$

$$\rho t = \frac{W}{Vt} \tag{4}$$

$$CCI = \frac{(\rho t - \rho b)}{\rho t} \times 100 \tag{5}$$

$$HR = \frac{\rho t}{\rho b} \tag{6}$$

Table 2
Factor level and experimental data for Box-Behnken design.

Run	Factor A (inlet air temp) °C	Factor 2 (feed flow rate) mL/min	Factor 3 (carrier to coating ratio)	Response 1 (Y1) (AOR)	Response 2 (Y2) (yield) %	Response 3 (Y3) (DL CUR) %	Response 4 (Y4) (DL QUE) %
1	(0) 110	(0) 18	(0) 9.522	30.9	51	97	97.9
2	(−) 105	(0) 18	(+) 13.33	48.9	50.3	95.9	97
3	(−)105	(−) 16	(0) 9.522	34.1	39	95.8	96.3
4	(+) 115	(+) 20	(0) 9.522	28.2	50	96.7	97.6
5	(+) 115	(0) 18	(−) 5.714	18.2	50.2	97.3	98.2
6	(0) 110	(−) 16	(−) 5.714	19.3	59	98.7	99.1
7	(−) 105	(+) 20	(0) 9.522	31.8	34	95.1	95.8
8	(0) 110	(0) 18	(0) 9.522	30.9	51	97	97.9
9	(+) 115	(−) 16	(0) 9.522	29.8	56	97.2	98.3
10	(−) 105	(0) 18	(−) 5.714	21.3	51	96.9	98
11	(0) 110	(0) 18	(0) 9.522	30.9	51	97	97.9
12	(0) 110	(+) 20	(+) 13.33	51.3	41	95.2	96.8
13	(0) 110	(0) 18	(0) 9.522	30.9	51	97	97.9
14	(0) 110	(0) 18	(0) 9.522	30.9	51	97	97.9
15	(0) 110	(+) 20	(−) 5.714	24	43	96.8	97.3
16	(+) 115	(0) 18	(+) 13.33	46.3	48	95	97
17	(0) 110	(−) 16	(+) 13.33	47.2	54	94.1	96.5

0; + and − refer to the 3 different levels of factors. (0) = Intermediate level; (−) = lower level (+) = higher level.

2.2.3. Design of experiments (DoE)

As per the industrial view point, the DoE plays an important role in optimization of various formulation and process variables which has a direct effect on the product quality and characteristics. It also plays a significant role in scaling up of manufacturing processes [39]. DoE turns out to be an efficient as well as cost-effective process for understanding the relationship among variables and to find critical factors influencing product quality [40]. The outcomes of solidification of L-SNEDDS specified that the Lf and micromeritic properties of PBs and GLEP in the ratio of 1:1 was almost comparable to A-200 which is the most widely accepted solid carrier. Hence, these were used as the solid carriers for DoE. Preliminary screening experiments were carried out for assessing the processing and formulation characteristics of S-SNEDDS. The outcomes from the preliminary screening experiments proposed that carrier to coating ratio (PBs + GLEP):A-200, feed flow rate and inlet air temperature were the chief factors influencing the characteristics of S-SNEDDS powder. Hence these three factors were run at 3 different levels i.e. −1, 0, and +1 (Table 2) and their effect on the responses such as drug loading, AOR and product yield. A set of 17 trials using Box Behnken design (BBD) was implemented to convert the L-SNEDDS into free-flowing powder using spray drying technology [41]. Initially the batches containing different carrier to coating ratios were prepared. A total of 17 different porcelain mortars were taken and L-SNEDDS preconcentrate (1 mL each) was added to each mortar. These were labelled from F1-F17. Further in each mortar 1 g of PBs and 1 g of GLEP was added as solid carriers and triturated slowly to permit uniform spreading of L-SNEDDS preconcentrate. In mortars containing F2, F12, F16 and F17 150 mg of A-200 was added to obtain formulations with a carrier to coating ratio 13.3. Similarly, A-200 (210 mg) was added in mortars containing formulations F1, F3, F4, F7, F8, F9, F11, F13, and F14 to obtain formulations with carrier to coating ratio of 9.52. In mortars containing formulations F5, F6, F10, and F15, A-200 (350 mg) was added to obtain formulations with carrier to coating ratio of 5.71. Each formulation was mixed for 5 min in order to obtain an even blend. Then the AOR, BD, TD, CCI and HR of each formulation were calculated prior to spray drying as per the equations given in Section 2.2.2.2 [38]. All the formulations were subjected to spray drying (Spray dryer; SprayMate, JISL, Navi Mumbai, India) by keeping the process variables for each batch as given in Table 2. In order to spray dry these formulations, water (100 mL) was used to make a dispersion. Spraying of these dispersions was carried out through spray nozzle with a diameter of 0.7 mm. The air pressure during the spray process was 4 Kg/cm^2.

2.2.4. Characterization parameters

The initial trial batches and optimized formulation were characterized by using following parameters.

2.2.4.1. Micromeritic properties. The AOR of different formulations (F1 to F17) and optimized SD formulation (SD-S-SNEDDS) were determined after spray drying and the results were compared with NSD product (NSD-S-SNEDDS). The procedure for determination of AOR is given in Section 2.2.2.2.

2.2.4.2. Drug loading. The percentage drug loading of all the prepared SD-S-SNEDDS (F1-F17, and optimized S-SNEDDS) was calculated. The SNEDDS loaded with CUR and QUE (10 mg each) were added in a beaker containing distilled water (500 mL). The beaker containing diluted SNEDDS was kept on a magnetic stirrer at 500 rpm. An aliquot (5 mL) was taken out from this dilution and centrifuged for 10 min at 10,000*g* (Centrifuge, REMI CM-12 PLUS, New Delhi, India). The clear liquid supernatant was taken out with the help of a micropipette and passed through a 0.2 μm syringe filter. The sample (20 μL) was injected to High-Performance Liquid Chromatography (HPLC; LC-20 AD; Shimadzu, Japan). The calculation of percentage loading of CUR and QUE was carried out as per Eq. (7) [9].

$$Drug\ Loading\ (\%) = \frac{Amount\ of\ drug\ in\ formulation}{Actual\ amount\ of\ drug\ added} \times 100 \quad (7)$$

2.2.4.3. Product yield. The percentage yield of each SD-S-SNEDDS trial batches (F1-F17) and optimized batch was calculated according to Eq. (8).

$$\%Yield = \frac{Final\ powder\ weight}{Initial\ weight} \times 100 \quad (8)$$

Here, final powder weight is the weight obtained after spray drying whereas initial weight is the weight of powder before spray drying [42].

2.2.4.4. Droplet size (DPS) and zeta potential (ZP) analysis. DPS and ZP of L-SNEDDS and SD-S-SNEDDS (optimized batch) were obtained using zeta sizer (ZS90, Malvern Instruments Ltd., UK). The samples were held in polystyrene cuvettes at 90 degree angle and then laser light with a potential of 50 mV was passed through the samples. An aliquot (0.1 mL) of SNEDDS sample was taken and added in a beaker containing 100 mL of d.w. It was passed through 0.2 μm syringe filter and 1 mL of filtrate was placed in sample cell and analyzed at 25 °C [38].

2.2.5. Characterization of optimized batch, raw drugs and excipients

2.2.5.1. DSC analysis. The DSC analysis was carried out for raw CUR, QUE, A-200, PB, GLEP, and optimized batch of SD-S-SNEDDS and NSD-S-SNEDDS powder (DSC 6000, PerkinElmer, Netherlands, USA). Each sample (3 mg) was placed and heated inside an aluminium crucible individually at a rate of 10 °C/min under nitrogen with a flow rate of 50 mL/min. The range for the thermograms of samples was kept 10 to 450 °C [41].

2.2.5.2. PXRD analysis. The PXRD patterns of raw CUR, QUE, A-200, PB, GLEP, and optimized formulation of SD-S-SNEDDS and NSD-S-SNEDDS were noted using an X-ray diffractometer (Bruker axs, D8 Advance) using Cu line as the radioactivity source. The samples were kept in the sample slot and pushed efficiently with iced glass. Then, samples were taken inside the PXRD instrument and the scanning speed was adjusted at 0.010°min^{-1}, over a 2θ range of 10–60 degrees, The beams of X-Ray at 40 kV voltage and 40 mA current were made incident on the sample [38].

2.2.5.3. SEM. The thorough morphological and shape appearances of optimized S-SNEDDS powder both SD and NSD along with raw CUR and QUE as well as other excipients (A-200, PB, GLEP) were examined using SEM (JSM6100, JEOL, New Delhi, India). Each powder was speckled homogeneously on one side of a twofold glue tape, fixed by aluminium stub on the other side. Gold sputter coater was used to coat the aluminium stab in a high vacuum evaporator. An augmented voltage of 10 kV was used for the scanning purpose [41].

2.2.6. Dissolution study

Dissolution study was carried using USP dissolution apparatus I, basket type (DS8000, Lab India, Mumbai, India), which was rotated at 100 ± 4 rpm. The temperature of 37 ± 0.5 °C was maintained during the experimentation. The raw CUR, raw QUE, L-SNEDDS and optimized S-SNEDDS (both SD and NSD) containing CUR and QUE equivalent to 10 mg each were added to each vessel individually containing the dissolution medium. The size "000" capsules (length: 2.61 cm, diameter: 0.99 cm) were taken and the above mentioned batches were added in these capsules separately. The dissolution study was carried in 900 mL of SGF (pH 1.2) for 60 min. At fixed time points (0.083, 0.16, 0.25, 0.5, 0.75 and 1 h) the samples were taken out and substituted by new dissolution media in order to perpetuate the sink condition. Centrifugation of the withdrawn samples was carried out at 10,000*g* for 15 min.

The clear supernatant was separated and filtered through 0.2 μm syringe filter and analyzed at 395 nm by injecting onto HPLC. The study was carried out 6 times and results were noted down in terms of mean ± S.D. [43].

2.2.7. Permeability studies

Caco2 cell monolayer was used for carrying out the permeability study. Twenty one days before performing the study, the cells were cultured on Trans well membrane made of polycarbonate having a length of 1.2 cm and pore size of 004 cm. The transepithelial resistance of 300 Ω/cm^2 was used. Before carrying the transcellular transport study, the cultured cells were cleaned using the Hank's balanced salt solution having a pH 6.5. Transport buffer (0.5 mL) was added in the apical side (A) of cells. Whereas, 1.5 mL of transport buffer was added in the basolateral side (B). To conduct the permeability study, raw CUR (10 mg) and raw QUE (10 mg) were weighed and a suspension of each drug was made separately using carboxy methyl cellulose solution (0.2% *w/v*). CUR and QUE loaded L-SNEDDS, CUR and QUE loaded SD-S-SNEDDS powder and CUR and QUE loaded NSD-S-SNEDDS powder each containing CUR and QUE 10 mg were added in a beaker containing 500 mL water. The aforementioned solutions (20 μM) were supplemented into the "A" and "B" sides of cell. The experiment was conducted for five hours. From B side of cell 0.1 mL sample was taken after each hour, up to 5 h and the volume which was taken out was substituted with equivalent volume of new transport buffer. Centrifugation of the withdrawn samples was carried out at 10,000*g* for 15 min. The analysis of the sample was done by passing the sample through syringe filter (0.2 μm) and then injecting onto HPLC at 395 nm. The amount of drug permeating through the membrane with respect to time was noted [9].

2.2.8. Accelerated stability studies

The optimized batch of SD-S-SNEDDS powder was kept in stability chamber (Remi electro technique, Mumbai, India) for 3 months at 40 °C ± 2 °C/75% R.H. ± 5%R.H. The outcomes of micromeritic properties, DS, drug loading and dissolution profile of fresh and aged samples were compared The obtained outcomes were statistically compared by ANOVA using GraphPad Prism version 7.0 (GraphPad Software Inc., CA, USA). In case the *P* value was <0.05 it indicated the difference was significant between the results of two or more groups. In case of dissolution studies model independent analysis (f2 comparison) was also used to compare the results. If the value was above 50, it indicated similar dissolution profiles of two groups whereas values less than 50 indicated dissimilar profiles [9].

2.2.9. Cell line toxicity study

MTT (3-(4,5-Dimethylthiazol-2-yl)-2,5-diphenyltetrazolium bromide) assay was carried out on the basis of viability of cells that release succinate dehydrogenase which reduces tetrazolium salt of MTT to produce formazan. Initially, the cell count was adjusted to 1.0×10^5 cells/mL by making suspension in DMEM (Dulbecco's Modified Eagle Medium) medium having 10% FBS (Fetal Bovine Serum). Then, the suspension was further cultured by adding 100 μL of suspension in 96 well plate for 24 h. Then cells were centrifuged at 9625*g* and pellets were suspended in different wells having serial dilutions in the maintenance media containing 100 μL each of raw CUR, raw QUE, raw CUR-QUE (1:1) mixture, CUR-QUE (1:1) SD-S-SNEDDS powders and placebo SNEDDS powders at concentrations of 25, 12.5 and 6.25 μg/mL and incubated at 37 °C for 48 h in the presence of 5% carbon dioxide. The placebo SNEDDS powders were taken as control to check the possible toxicity of excipients. After 48 h sample solutions were centrifuged at 9625*g* and pellets were re-suspended in MEM-PR solution containing 20 μL of MTT and incubated at 37 °C in the presence of 5% v/v carbon dioxide. After 2 h, 100 μL of DMSO was added to dissolve the formed formazan and absorbance was noted at 540 nm [44]. The percentage viability of cells was calculated using formula given in Eq. (9).

$$\%cell\ viability = \frac{Mean\ OD\ of\ individual\ testgroup}{Mean\ OD\ of\ control\ group} \times 100 \quad (9)$$

where OD is optical density.

3. Results and discussions

3.1. Screening of solid carriers

All the individual carriers as well as combinations prepared using PBs and GLEP in three different ratios were evaluated for micromeritic properties. The value of Lf for solidifying L-SNEDDS preconcentrate (1 g) for PB, GLEP, A-200, PVA, HPMC, MCC PH102, lactose, GLEP -PB (1:1), (1:2), (2:1), was 0.14 (7.14 g), 0.11 (9.09 g), 1.42 (0.7 g), 0.2(5 g), 0.25 (4 g), 0.2 (5 g), 0.16 (6 g), 0.41 (2.43 g), 0.29 (3.44 g), 0.35 (2.85 g) respectively. The more the Lf value means less amount of carrier is required for transformation of L-SNEDDS preconcentrate into solid powder with free flowing properties [45]. The Lf value was found to be highest in case of A-200 followed by GLEP and PB combination. It was noted that when PB or GLEP were used alone, both exhibited a reduction in the value of Lf in comparison to their combination. The AOR, HR, BD, TD and CI for all these batches prepared using different carriers are presented in Table 1. The carriers which were used for formulation of L-SNEDDS presented greater variation in their micromeritic properties. The range of AOR was found between 20.00 θ (A-200) to 56.83 θ (HPMC). The value of TD was found to be in the range of 0.104 g/cm^3 (A-200) to 0.78 g/cm^3 (PB-GLEP in 2:1 ratio). Likewise, the range of BD was noted between 0.092 g/cm^3 (A-200) to 0.50 g/cm^3 (PB). In case of CI the range was noted between 19 (MCC PH102) and 54 (GLEP + PB 2:1). The HR was found in the range of 1.16 (A-200) to 2.5 (GLEP + PB 2:1). These changes in the micromeritic characteristics of different carriers can be attributed to differences in their physicochemical properties as well as their Lf. The excellent flow rate, TD, BD, HR, CI were seen in case of A-200 as compared to all other carriers used, due to its flocculent property and bigger surface area [19]. In contrast, PB-GLEP in the ratio of 2:1 exhibited least flow rate and increased density values. However, the prime purpose of this work was to explore the use of GLEP and PBs as carriers to solidify SNEDDS in order to get their dual benefits i.e., as an excipient and nutraceutical. Hence PBs and GLEP combination was expected to have good micromeritic properties in order to pass themselves as carriers. When the various combinations of PBs-GLEP (i.e. 1:1, 1:2 and 2:1) were used then they failed to comply with the requirement as the AOR obtained was above 40 in all ratios. Hence, it was thought to add minimum amount of A-200 in the PB-GLEP combination as coating material. It is important to note that among the three combinations of PB-GLEP used the ratio of 1:1 was found better in terms of micromeritic properties. Hence this ratio was further explored by varying the amount of A-200 (i.e. carrier to coating ratio). The exact ratio was optimized through DOE that is discussed in subsequent section.

3.2. Examination of formulations of process variables

Conferring to BBD, a total of 17 trials were carried out in order to check the effect of carrier to coating ratio and different parameters of spray drying effecting the responses viz. AOR (Y1), product yield (Y2), drug loading of curcumin (Y3) and drug loading of quercetin (Y4). The responses for these 17 trials are summarized in Table 2. The maximum AOR (Y1) (51.3 θ) was found for run 12 while least (18.2 θ) for run 5. Likewise, for Yield (Y2) run 6 showed the maximum value of 59% and run 3 showed a minimum value of 39%. In case of drug loading of curcumin (Y3), run 6 showed a maximum value of 98.7%. Whereas, run 17 showed a minimum value of 94.1%. Run 6 showed a maximum value for drug loading (99.1%) of quercetin (Y4) and a minimum value for run 7 (95.8%). The ratio of maximum to minimum for Y1, Y2, Y3 and Y4

Table 3
Fit summary and ANOVA using DOE tools.

Summary

Source	Sequential *P* value				Lack of fit *P* value				Adjusted R-squared			
	Y1	Y2	Y3	Y4	Y1	Y2	Y3	Y4	Y1	Y2	Y3	Y4
Linear	<0.0001	0.0207	0.0040	0.0050	0.056	0.075	0.083	0.069	0.9378	0.4045	0.5430	0.5267
2FI	0.9983	0.9911	0.1956	0.6777	0.017	0.063	0.011	0.031	0.9195	0.2336	0.6207	0.4678
Quadratic	0.0165	0.4172	0.2158	0.1737	0.097	0.047	0.030	0.018	0.9711	0.2518	0.7023	0.6102
Cubic	–	–	–	–					1.0000	1.0000	1.0000	1.0000

Source	Predicted R-squared				F-value				*P* value			
	Y1	Y2	Y3	Y4	Y1	Y2	Y3	Y4	Y1	Y2	Y3	Y4
Linear	0.9032	0.2832	0.3542	0.3554	81.46	4.62	7.34	6.94	<0.0001	0.0207	0.0040	0.0050
2FI	0.7783	−1.3138	0.0822	−0.4634	0.0111	0.0339	1.89	0.5205	0.9983	0.9911	0.1956	0.6777
Quadratic	0.7979	−4.2377	−1.0838	−1.7284	6.97	1.08	1.91	2.22	0.0165	0.4172	0.2158	0.1737
Cubic	0.9032	0.2832	0.3542	0.3554								

Sequential model sum of squares (type 1)

Source	Sum of squares				Df				Mean square			
Mean vs total	40,572.37	5670.01	1.582E+05	1.617E+05	1	1	1	1	18,112.59	40,572.37	1.582E+05	1.617E+05
Linear vs mean	324.00	178.81	12.56	6.90	3	3	3	3	521.16	108.00	4.19	2.30
2FI vs linear	3.06	183.55	2.68	0.5825	3	3	3	3	0.0917	1.02	0.8942	0.1942
Quadratic vs 2FI	95.19	193.42	2.13	1.82	3	3	3	3	20.70	31.73	0.7116	0.6059
Cubic vs quadratic	205.50	73.44	2.60	1.91	3	3	3	3	6.93	68.50	0.8675	0.6375
Residual	0.0000	59.25	0.0000	0.0000	4	4	4	4	0.0000	0.0000	0.0000	0.0000
Total	41,200.13	6358.47	1.582E+05	1.617E+05	17	17	17	17	1162.31	2423.54	9304.35	9512.65

Lack of fit test

Source	Sum of squares				Df				Mean square			
Linear	83.17	303.76	50.30	4.31	9	9	20	9	9.24	33.75	0.8244	0.4792
2FI	82.89	300.70	29.91	3.73	6	6	14	6	13.82	50.12	0.7896	0.6217
Quadratic	20.80	205.50	19.83	1.91	3	3	10	3	6.93	68.50	0.8675	0.6375
Cubic	0.0000	0.0000	0.9058	0.0000	0	0	2	0	0.0000	0.0000	0.0000	0.0000
Pure error	0.0000	0.0000	0.0000	0.0000	4	4	4	4	0.0000	0.0000	0.0000	0.0000

Model summary statistics

Source	Std. Dev.				R^2				Adjusted R^2			
Linear	2.53	4.83	0.7555	0.5760	0.9495	0.5161	0.6287	0.5497	0.9378	0.4045	0.5430	0.5267
2FI	2.88	5.48	0.6883	0.6108	0.9497	0.5210	0.7629	0.3875	0.9195	0.2336	0.6207	0.4678
Quadratic	1.72	5.42	0.6097	0.5227	0.9874	0.6726	0.8698	0.8942	0.9711	0.2518	0.7023	0.6102
Cubic	0.0000	0.0000	0.0000	0.0000	1.0000	1.0000	1.0000	0.9623	1.0000	1.0000	1.0000	1.0000

Model summary statistics

Source	Predicted R^2				PRESS				Adjusted R^2			
Linear	0.9032	0.2832	0.3542	0.3554	159.48	613.62	14.09	8.37	–	–	–	–
2FI	0.7783	−1.3138	0.0822	−0.4634	365.12	1452.51	18.34	16.41	–	–	–	–
Quadratic	0.7979	−4.2377	−1.0838	−1.7284	332.76	3288.04	41.64	30.60	–	–	–	–
Cubic	0.5462	−1.1234	−1.0982	−1.0003	120.23	1015.22	7.356	10.22	–	–	–	–

were 2.81, 1.51, 1.04 and 1.03, respectively. The power of transformation was not required since all the values of maximum to minimum ratio were below 10. DoE tools (lack of fit test, sequential model sum of squares, and model summary statistics) were used for carrying out the statistical analysis of the model. Table 3 summarizes the results obtained for responses using these tools. The lower value of standard deviation and predicted residual error sum of square (PRESS), high value of R-square and $P < 0.0001$ recommended to choose linear model for all responses except. In case of Y1 quadratic model was suggested. ANOVA was used for the analysis of obtained results which are presented in Table 3. The F value for all responses was found as follows: Y1: 6.97, Y2:4.62, Y3:7.34 and Y4:6.94. The *P* value was found less than 0.05 in all cases demonstrating significance of model. In addition the adequate precision values was found to be greater than 4 (Y1:24.04, Y2:7.45, Y3:8.18 and Y4:8.85) This specified that the used model is adequate. For all responses the R-squared value was found above 0.500. It was concluded from all the obtained ANOVA results that the responses have responded significantly to the independent variables.

Eqs. (10) to (13) present the polynomial equation for different response

$$\textbf{\textit{AOR}}: \mathrm{Y1} = +30.90 - 1.70{*}\mathrm{A} + 0.6125{*}\mathrm{B} + 13.86{*}\mathrm{C} + 0.1750{*}\mathrm{AB} + 0.1250{*}\mathrm{AC} - 0.1500{*}\mathrm{BC} - 0.850{*}\mathrm{A}^2 + 0.9250{*}\mathrm{B}^2 + 3.62{*}\mathrm{C2} \quad (10)$$

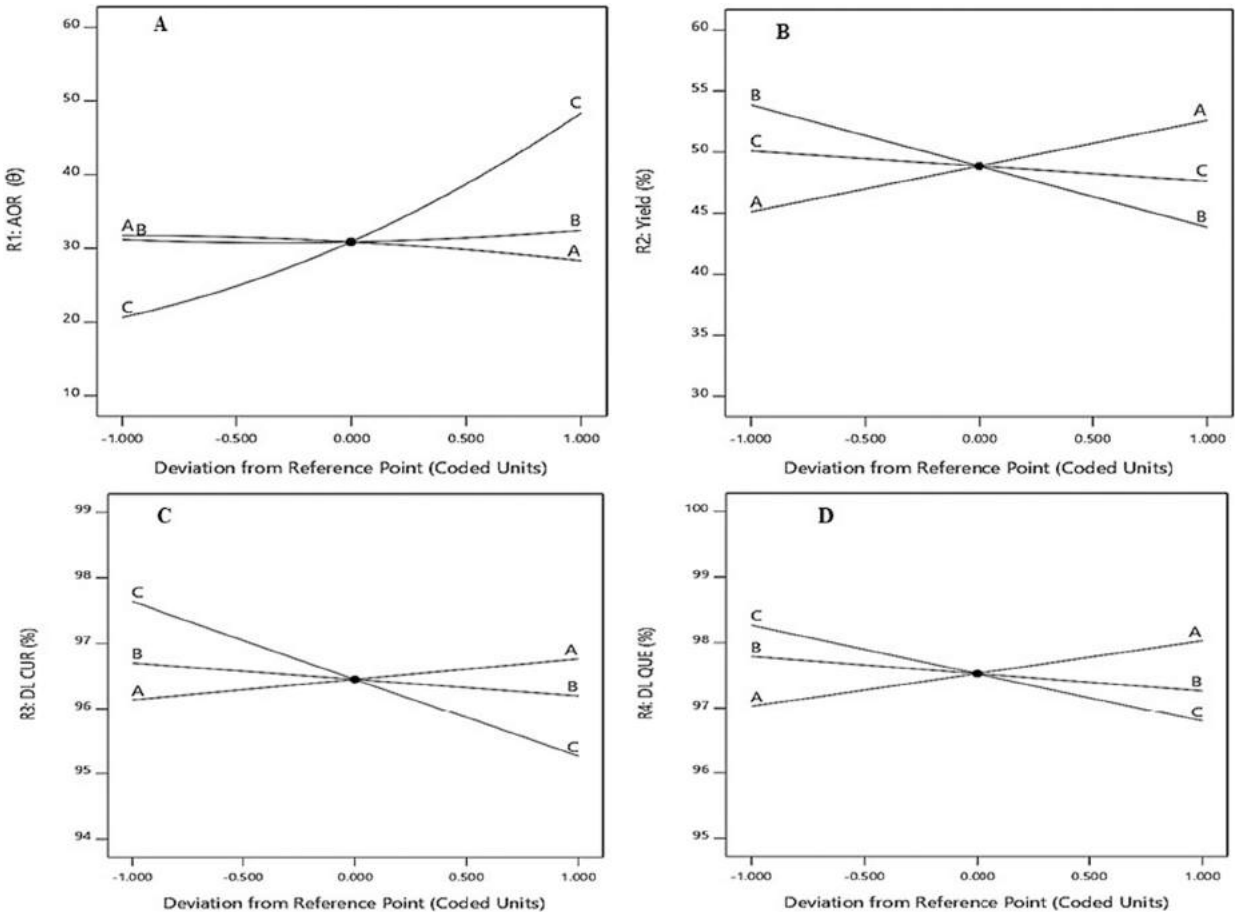

Fig. 1. Perturbation plots showing effect of different variables on **A)** AOR; **B)** %Yield; **C)** drug loading of CUR; **D)** drug loading of QUE.

$$\textbf{Yield}: Y2 = +48.85 + 3.74*A - 5.00*B - 1.24*C \quad (11)$$

$$\textbf{Loading of curcumin}: Y3 = +96.45 + 0.3125*A - 0.2500*B - 1.19*C \quad (12)$$

$$\textbf{Loading of quercetin}: Y4 = +97.53 + 0.5000*A - 0.2625*B - 0.7375*C \quad (13)$$

In case the sign is positive in the above equations, it stated that a synergistic effect of factors was obtained on the responses. In case the sign is negative it specified that the factors re having an antagonistic effect on the responses. For AOR (Y1) an increase in value was noted as the carrier to coating ratio (Factor C) was increased whereas, all other factors showed a reduction in value with increase in carrier to coating ratio. An increase in Yield (Y2), loading of curcumin (Y3), loading of quercetin (Y4) was noted with an increase in inlet air temperature (Factor A). Whereas, AOR showed a decrease in value with an increase in inlet air temperature (Factor A). The yield (Y2), loading of curcumin (Y3), and loading of quercetin (Y4) were found to be decreased as the feed flow rate (Factor C) increased. However, AOR showed an increase in its value with increase in feed flow rate. Besides the polynomial equation, the determination of power of factors on the responses is also important to be recognized. In spite of having a particular effect (antagonistic or synergistic) of factors on responses, the effect may not be much significant.

Despite having antagonistic or synergistic effect of factors on responses, the effect may not be so significant. The significance of the effect of different factors on responses is understood evidently by the perturbation plot. The perturbation plot graphs for all factors are shown in Fig. 1. From Fig. 1A, it was noted that factor C is the main dominating factors affecting AOR whereas factor A and B have negligible effect on AOR. Fig. 1B revealed that product yield was mostly affected by both factors A and B equally whereas, factor C has minimum effect on product yield. In case of drug loading for CUR, factor C has played the most dominant role whereas the factors A and B have the minimum role in this case as indicated in Fig. 1C. In case of drug loading for QUE, factor A and C had the most dominant effect and factor B was having the least effect as indicated from Fig. 1D.

The polynomial equations aided in generation of 3-D response surface plots that further facilitated to know the design. The contour graphs presented in Fig. 2 deciphers that as carrier to coating ratio increased the AOR also increased. As the carrier to coating ratio increased amount of A-200 reduced. A-200 acted as an adsorbent that adsorbed the moisture from the sample, decreasing the accumulation of the particles, hence reducing the AOR at higher concentration of A-200 (reduced carrier to coating ratio). The inlet air temperature had a synergistic effect on yield (Y2), loading of curcumin (Y3), loading of quercetin (Y4). Whereas AOR (Y1) showed a decrease in value with an increase in inlet air temperature (Factor A).

The feed flow rate had an antagonistic effect on the yield (Y2), loading of curcumin (Y3), and loading of quercetin (Y4). However, AOR showed an increase in its value with increase in feed flow rate. When the inlet temperature increased the powder sample got dried more effectively and this reduced particle agglomeration, decreasing the angle of repose. The feed flow rate is the quantity of fluid passing through a given cross sectional area per unit time. Thus, if the feed flow rate is more, the quantity of liquid passing through the orifice will be more. Hence, incomplete drying happens causing particle agglomeration and presence

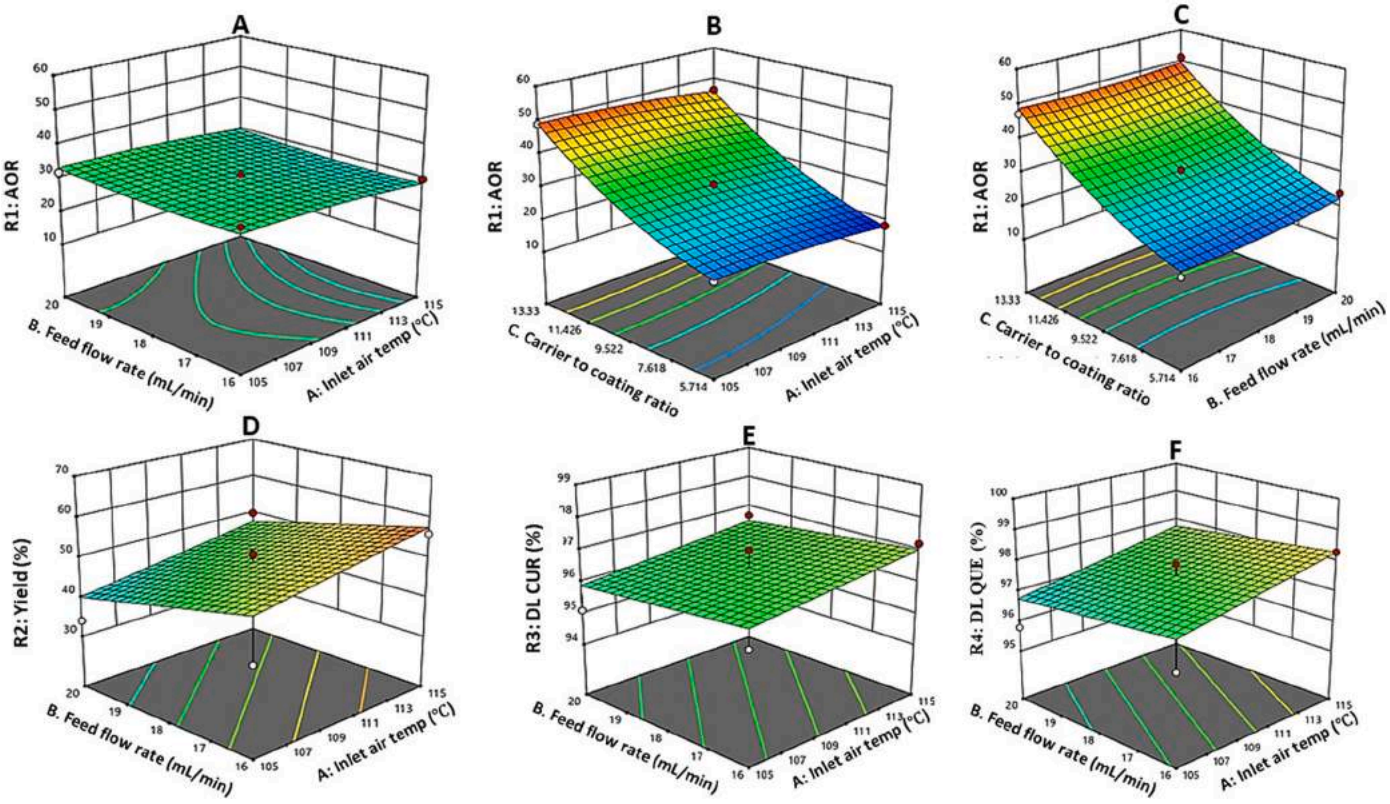

Fig. 2. 3D response surface plots for effect of A) factors A&B; B) A&C; C) B&C on AOR; for factors A&B on D) yield; E) drug loading of curcumin; F) drug loading of quercetin.

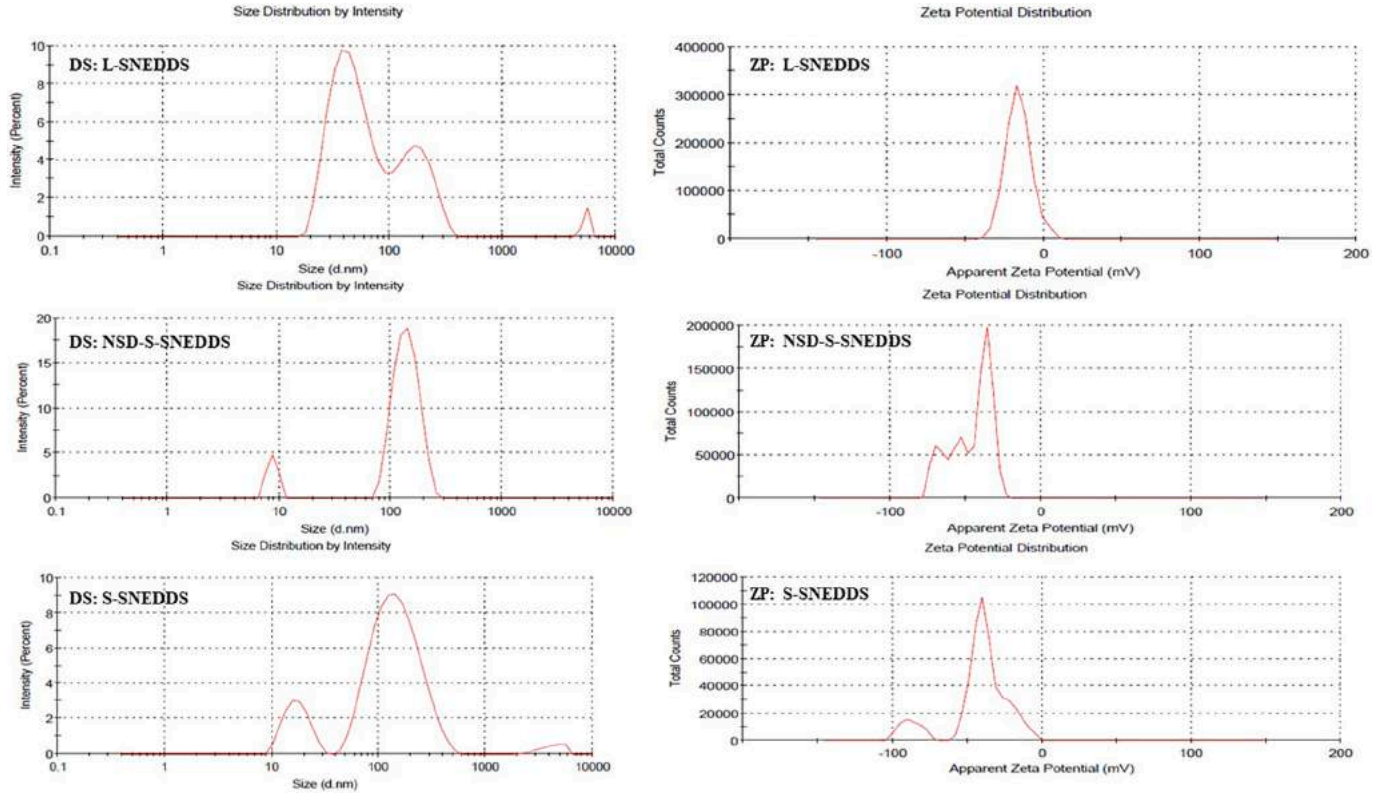

Fig. 3. Results of average DS and ZP of L-SNEDDS, NSD-S-SNEDDS and SD-S-SNEDDS.

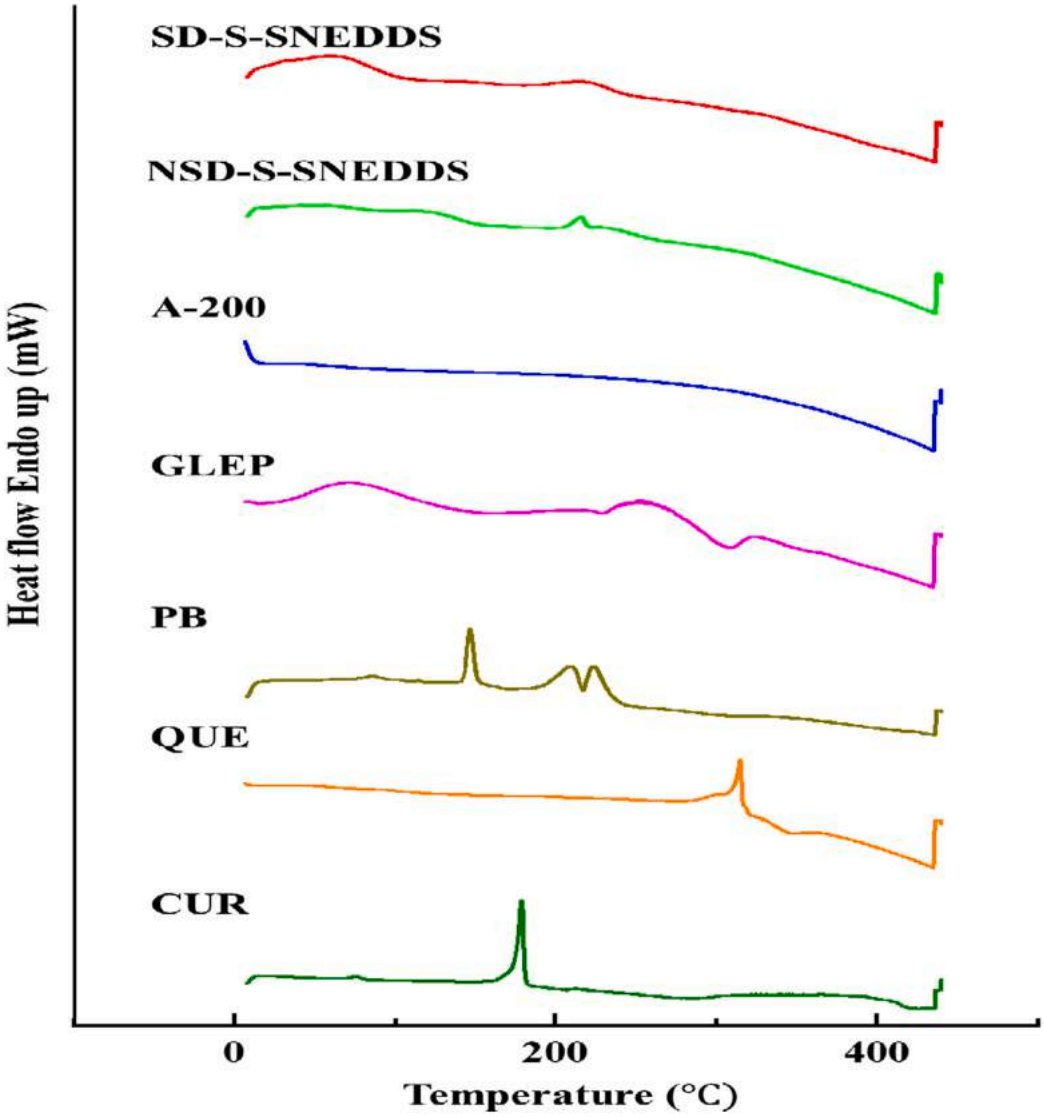

Fig. 4. DSC thermograms of CUR, QUE and developed formulations.

of moisture which ultimately reduces AOR. The contour plots as presented in Fig. 2 shows that A-200 content, and inlet temperature have a synergistic effect whereas feed flow rate has an antagonistic effect on product yield. A-200 is a solid porous carrier. Furthermore, it intensified feed viscosity leading to a decrease of the radial speed and reducing the tackiness of the powder inside the chamber eventually yielding a larger quantity of the product at the collection site. As the inlet temperature increased faster and effective drying of the feed occurred by effective evaporation of moisture leading to a higher production of the resultant product. Increasing the feed flow rate has an antagonistic influence on product yield as higher feed flow rate reduced the speed of heat and mass transfer. Additional reason could be that at increased flow rate, some part of the feed did not get atomised and it travelled straight to the chamber. Thus, it enhanced the ratio of product waste to product yield [43,46].

3.3. Graphical optimization

In order to find out the levels of factors A–C, graphical optimization of formulation was carried out which showed Y1 (AOR) in the range of 12.9 θ to 22.9 θ; Y2 (Yield) in the range of 48.5 to 69%; Y3 (drug loading of curcumin) in the range of 96.6 to 99.8% and Y4 (drug loading of quercetin) in the range of 97.8 to 100.2%, respectively. The predicted values obtained through BBD for the three factors were 115 °C (A), 20 mL/min (B), and 5.71 (C). By utilizing the recommended values of factors on optimized batch of S-SNEDDS was prepared. The experimental value of AOR was 22.1 θ, Yield was 56%, drug loading of curcumin was 97.3% and drug loading of quercetin was 98.1%. These values were near to the predicted values (i.e. Y1 = 17.97 θ; Y2 = 58.8%; Y3 = 97.2%; Y4 = 98.0%). This specified the reproducibility of optimization method.

3.4. Characterization of optimized formulation

3.4.1. DPS and ZP

The results revealed that the average DPS of prepared L-SNEDDS was 63.46 ± 2.12 nm and average ZP −14.8 ± 3.11 mV. The polydispersity index (PDI) of L-SNEDDS was 0.43. Upon solidification the average DPS was found to be 98.76 ± 3.22 nm, average ZP was found to be −45.9 ± 1.98 mV, and PDI 0.57 for NSD-S-SNEDDS. The results of droplet size and zeta potential are shown in Fig. 3. The main reason for enhancement in negative charge is the adsorption of L-SNEDDS on the surface of negatively charged GLEP and PBs. The Gram positive bacteria present in PBs contain negative charge in their cell wall due to presence of teichoic acids linked to either the peptidoglycan or, to the underlying plasma membrane [47,48]. Furthermore, polysaccharide contains number of –

OH groups that provide negative charge on them [49]. Although A-200 also provides some positive electrostatic charge but its impact was significantly less on the ZP of SD-S-SNEDDS. The average DPS got reduced after spray drying (70.08 ± 3.15 nm) with PDI of 0.56 and ZP was almost unaffected (−42.6 ± 1.58 mV) as observed for SD-S-SNEDDS. It is pertinent to mention here that the upper shift of ZP to larger values specifies improved formulation stability [9]. Upon solidification the DPS got increased since the liquid droplets got adsorbed on solid carrier in aqueous medium in case of NSD-S-SNEDDS as well as SD-S-SNEDDS. Interestingly the DPS of SD-S-SNEDDS was found less as compared to NSD-S-SNEDDS owing to the impact of spray drying which resulted in size reduction as well as achievement of un-agglomerated free flowing powder. The PDI of the prepared SNEDDS were found slightly high indicating inhomogenous distribution. However, for a lipid based formulation for oral delivery, it was found within the limit of 0.05–0.7, indicating acceptable size distribution [50]. The normal range for PDI should be between 0 and 10 [51].

The droplet size distribution is a critical factor in SNEDDS for drug absorption and colloidal stability. The smaller droplet size provides large interfacial surface area, which increases the drug absorption and provides excellent colloidal stability and vice versa [52]. Furthermore, the droplet size also has influence on the oxidative stability of o/w nanoemulsions. It has been observed that the o/w emulsions with smaller droplet size have lower residual oxygen contents than those of the larger droplet size emulsions [53]. Thus, the SNEDDS with lower droplet size provide very good stability to compounds like curcumin and quercetin. Zeta potential plays an important role in characterizing charge on the nanoformulations and understanding their physical stability [54]. Higher positive or negative value of ZP indicates excellent physical stability of nanoformulations due to electrostatic repulsion of individual particles. The minimum value of ±30 mV zeta is generally considered to have sufficient repulsive force to attain better physical colloidal stability [55–57]. Whereas, a small value of zeta potential may cause particle aggregation and flocculation due to the van der Waals attractive forces that act upon them and may result in physical instability [58].

In some of the previous studies carried out by various researchers on SNEDDS, either the DPS was found more or ZP was found less as compared to the developed SNEDDS in the present study, indicating its superiority. For instance, Kumar et al. developed S-SNEDDS loaded with CUR and duloxetine having mean DPS of 113.14 nm and ZP of −13.2 mV [38]. Similarly, in other study Joshi et al., formulated liquid SNEDDS for oral delivery of CUR for treating neuropathic pain having mean DPS of 213.7 nm [59]. Kazi et al., developed SNEDDS of curcumin and piperine having DPS ranging between 51 and 701 nm and ZP ranging between −10.6 mV and −36.4 mV [60]. Shukla et al., developed L-SNEDDS of curcumin for anticancer activity wherein, the DPS was 83.27 nm with ZP of −16 mV [61]. Similarly, some SNEDDS have been developed for QUE also, for example, Tran et al. reported quercetin SNEDDS with DPS of 208.8 nm and ZP of −26.3 mV [62]. In another study, Ahmad et al., developed QUE loaded L-SNEDDS with DPS of 94.63 nm and ZP of −17.91 mV [63]. In another study Ahmed et al., developed SNEDDS of QUE for its hepatoprotective activity against paracetamol induced hepatotoxicity, wherein the DPS of SNEDDS was ranging between 119 and 635 nm [64]. In the present study, the values of DPS ranged between 63 and 99 nm that indicated comparatively lower mean DPS and ZP of S-SNEDDS was found in the range of −42.6 to −45.9 mV, indicating towards better absorption and oxidative stability of formulations as compared to previously reported SNEDDS of QUE and CUR. Furthermore, it also indicates that developed SNEDDS were found superior in terms of previously reported formulations.

3.4.2. DSC

The DSC curves of raw CUR, raw QUE, PB, GLEP, A-200, and S-SNEDDS (SD and NSD) formulations are shown in Fig. 4. The peaks of pure CUR showed a sharp endothermic peak at 174.37 °C and for QUE a sharp endothermic peak was obtained at about 315 °C. The peaks corresponded to their melting points indicated their crystalline nature. In case of A-200 and GLEP flat line without any melting endotherm was seen owing to their liquid/amorphous nature. Whereas, in case of PBs a sharp endothermic peak was seen at around 140 °C. It is essential to note that in case of S-SNEDDS formulations the drug endothermic peaks were not present. This displayed that both the drugs have been completely dissolved in the formulation. Moreover, the oil-surfactant-co-surfactant system has provided adequate stabilization to the drug, because if the drugs would have been precipitated in the formulation then it would have led to appearance of crystalline peaks for both drugs. Furthermore, adsorption of CUR and QUE loaded L-SNEDDS on amorphous A-200, PBs and GLEP through spray drying further led to a complete amorphous state of the formulation. In order to have well understanding, the DSC outcomes were correlated with PXRD studies.

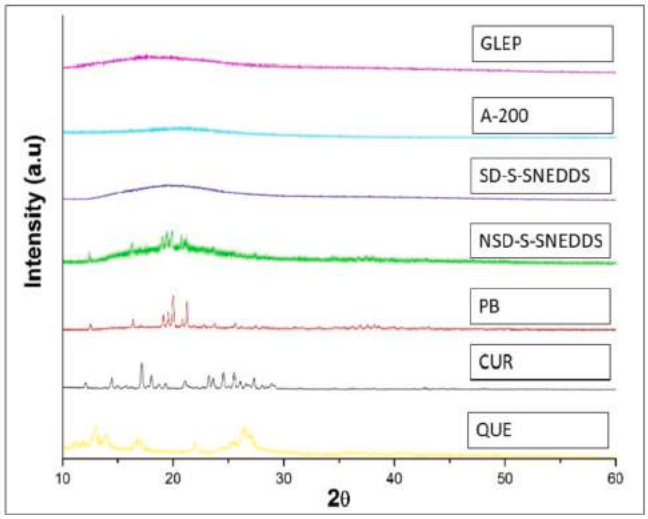

Fig. 5. PXRD patterns of CUR, QUE and developed formulations.

3.4.3. PXRD studies

Similar to the results of DSC, sharp crystalline peaks were observed for CUR and QUE whereas the other carriers used in the formulation as well as the prepared S-SNEDDS showed absence of crystalline peaks indicating the amorphous nature of carriers and complete solubility of drug in the liquid followed by their successful adsorption on the carriers. The results of PXRD are presented in Fig. 5. CUR, QUE and PBs had shown sharp peaks, revealing a characteristic crystalline pattern. In contrast, A-200 and GLEP did not show any intrinsic peaks owing to their amorphous nature. In case of PXRD of S-SNEDDS (SD and NSD), the crystalline peaks of raw CUR and QUE were absent, representing their amorphous pattern. Hence, similar to DSC outcomes, both CUR and QUE were present in a transformed amorphous state in the SNEDDS formulations prepared with GLEP and PBs as carriers and A-200 as coating agent.

3.4.4. SEM

The SEM images of raw CUR, raw QUE, PB, GLEP, A-200, NSD-S-SNEDDS and SD-S-SNEDDS are shown in Fig. 6a–g. CUR (Fig. 4a) and QUE (Fig. 6b) revealed crystalline structure presented by elongated blade like structures having sharp edges [9,65]. QUE appeared as long, cylindrical, structure with smooth surface [66]. The structure of GLEP (Fig. 6c) appeared to be extended, striated, quadrilateral structure with absorbent and uneven reticulated surface. The structure of PBs appeared as elongated with spongy and coarse surface and asymmetrical and reticulated boundaries (Fig. 6d). In case of A-200 the structure was observed to be extremely absorbent and even surface representing its shapeless nature (Fig. 6e). The NSD-S-SNEDDS powder appeared as

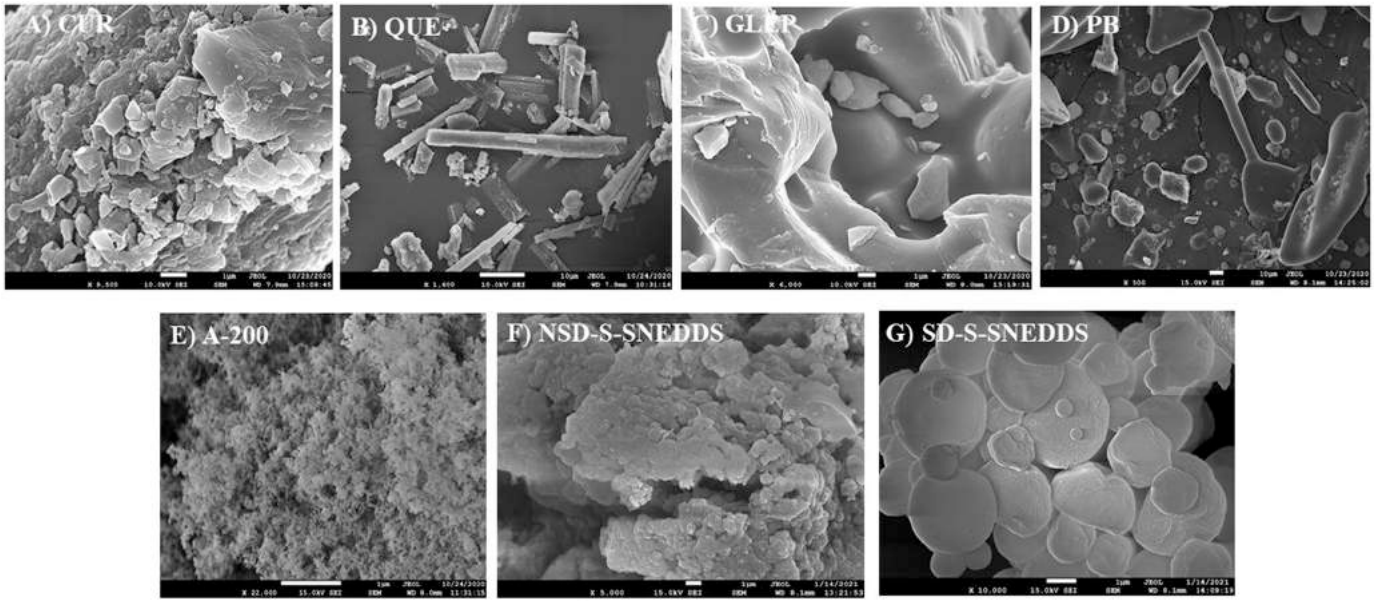

Fig. 6. SEM images of A) CUR; B) QUE; C) GLEP: D) PB; E) A-200; F) NSD-S-SNEDDS; G) SD-S-SNEDDS.

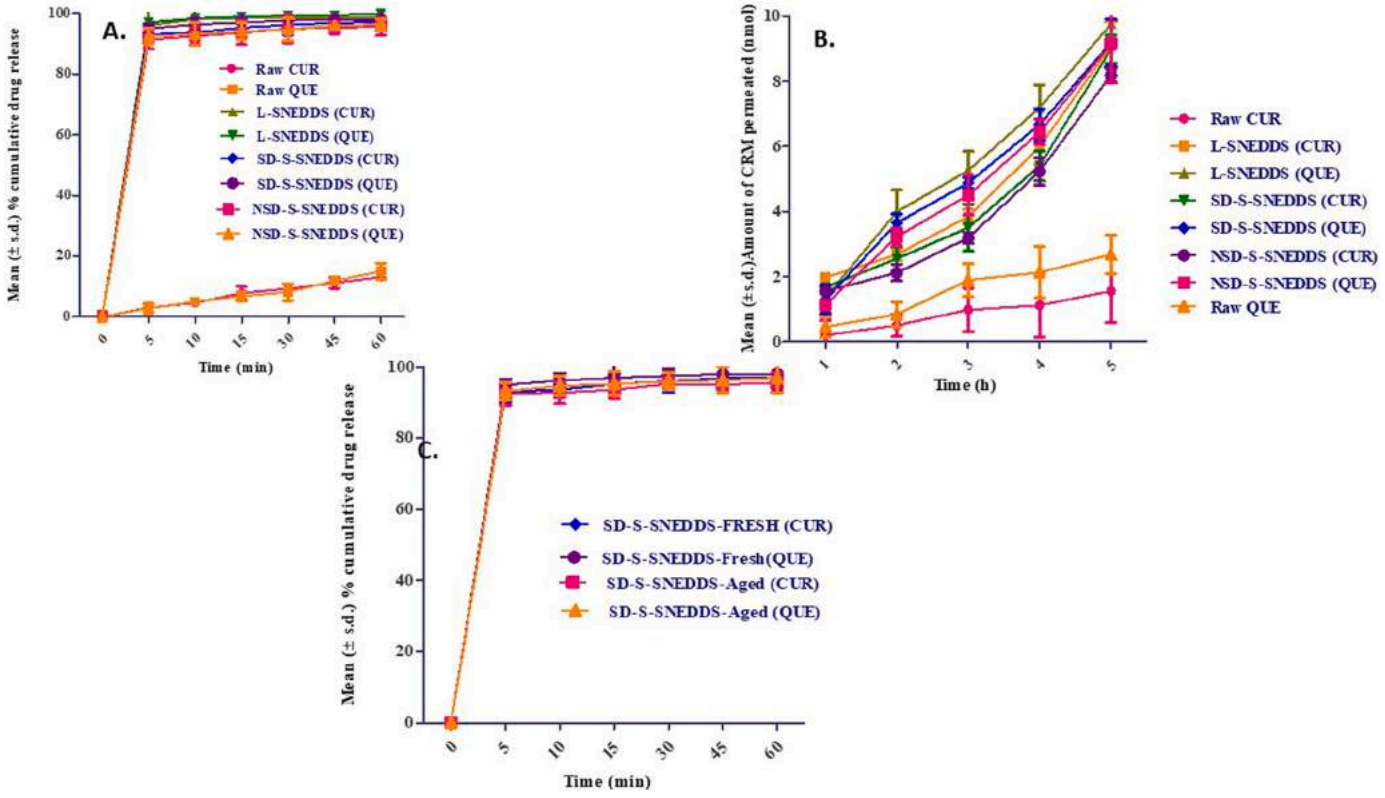

Fig. 7. A) Dissolution profile B) permeability profile C) stability profile of raw CUR, QUE and different SNEDDS formulations.

uneven surface subdivisions with spongy and bendable appearance signifying the occurrence of adsorbed L-SNEDDS isotropic mixture on the adsorbent surface of carriers, particularly A-200 and GLEP (Fig. 6f). Upon spray drying, the SD-S-SNEDDS appeared as even, un-agglomerated, absorbent, spongy and round with nonappearance of any bendable structure (Fig. 6g). The results of SEM were found to be similar to the PXRD and DSC outcomes for the S-SNEDDS formulation. Furthermore, the observed outcomes of SEM for S-SNEDDS sample has given grounds for enhanced flow characteristics for SD-S-SNEDDS in comparison to NSD-powder (as discussed in Section 3.1). The spray drying process of S-SNEDDS provided improved interaction between the spongy amorphous carriers and the liquids during the process of drying. Moreover, throughout drying, the humidity remaining inside the carriers also got evaporated and hence better void spaces were generated for liquid preconcentrate's adsorption. The general consequence was a non-agglomerated, free flowing, round, and porous-sponge like, S-SNEDDS formulation which can further be simply stored in any ampule/capsules or, can even be converted into solid dosage forms such as

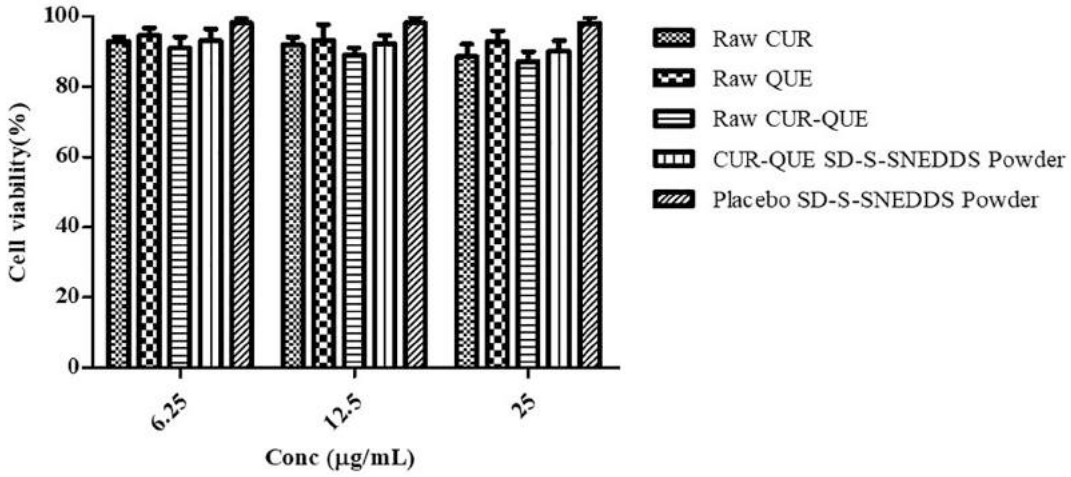

Fig. 8. Results of cell viability of unprocessed drugs, placebo and SNEDDS formulation.

spheroids or tablets. Comparable results were seen in earlier studies wherein the spray drying process for L-SNEDDS was carried out [38,43,67].

3.5. Dissolution study

From the in vitro dissolution study it was seen that drug release for both CUR and QUE was more than 90% during the initial 5 min from L-SNEDDS, NSD and SD-S-SNEDDS however, the drug release in case of both drugs in their raw form was only up to 20% in 60 min (Fig. 7A). There were about 4.5 folds enhancement in the dissolution rate of CUR as well as QUE when both the drugs were loaded into SNEDDS. This can be attributed to the reason that both drugs got solubilized completely by loading into emulsion. F2 value and one-way ANOVA was used to compare the release profiles of raw CUR, raw QUE, L-SNEDDS and S-SNEDDS. The *p*-values were noted to be less than 0.0001 and f2 values were less than 50 between raw CUR/QUE and their SNEDDS formulations i.e. L-SNEDDS, SD-S-SNEDDS and NSD-S-SNEDDS suggesting significant difference in the release of both drugs upon loading into SNEDDS. The p-values between L-SNEDDS versus its solid formulations were found above 0.05 [i.e. 0.908 (CUR) and 0.938 (QUE) for SD-S-SNEDDS as well as 0.858 (CUR) and 0.851 (QUE) for NSD-S-SNEDDS] indicating similar dissolution profiles. Similarly the f2 values between L-SNEDDS versus SD-S-SNEDDS were found above 50 [i.e. 57.68 (CUR) and 66.90 (QUE)] indicating no change in dissolution profiles of both the drugs upon their solidification using spray drying. However in case of NSD-S-SNEDDS the dissolution profile was found slightly less as compared to L-SNEDDS that was indicated by their f2 values (i.e. 49.07 (CUR) and 48.29 (QUE)) that were slightly less than 50. The outcomes of overall statistical analysis indicated the potential of spray drying in solidifying L-SNEDDS into solid free flowing powder without altering the release behavior of drugs. The slight decrease in dissolution profiles of both the drugs in case of NSD-S-SNEDDS could be inferred to agglomerated powders that can be confirmed through AOR and SEM studies.

3.6. In vitro cell line permeability studies

The main aim of this work was to estimate the CUR and QUE transport across the intestinal membrane through the developed SD-S-SNEDDS powder. As presented in Fig. 7B, it was noted that L-SNEDDS, SD-S-SNEDDS and NSD-S-SNEDDS showed a 5.82, 5.76 and 5.25 folds increased permeation of CUR in comparison to the raw CUR respectively at 5 h. In case of QUE, it was noted that L-SNEDDS, SD-S-SNEDDS and NSD-S-SNEDDS showed 3.39, 3.42 and 3.41 folds increased permeation of QUE in comparison to the raw QUE respectively at 5 h. The *P* values for drug's permeation between raw CUR and various SNEDDS formulations viz. L-SNEDDS, SD-S-SNEDDS and NSD-S-SNEDDS were found to be 0.0189, 0.0276 and 0.0324 respectively. Similarly the *P* values between raw QUE and various SNEDDS formulations viz. L-SNEDDS, SD-S-SNEDDS and NSD-S-SNEDDS were found to be 0.029, 0.035 and 0.048 respectively which were less than 0.05. This value of p which was less than 0.05 demonstrated remarkable improvement in permeability of both the drugs upon formulating SNEDDS. The *P* values between L-SNEDDS vs SD-S-SNEDDS and NSD-S-SNEDDS were 0.87 and 0.71 for CUR and 0.85 and 0.76 for QUE, which were above 0.05, demonstrating non-significant difference in drug's permeation upon solidification of L-SNEDDS. Many studies have established the potential of SNEDDS to enhance the intestinal lymphatic transport of the lipophilic drugs [68,69]. The present research work also verified that transportation of BCS class 4 (CUR) and BCS class 2 (QUE) drugs is enabled by loading it onto SNEDDS.

3.6.1. Stability studies

The mean DPS of SD-S-SNEDDS powder (aged) was found to be 75.33 ± 1.66 while, the DPS of fresh SD-S-SNEDDS formulations was 70.08 ± 1.09 nm. Likewise, the drug loading for fresh S-SNEDDS was 97.2 ± 3.32% for CUR and 98 ± 4.02% for QUE and for aged S-SNEDDS, it was 96.38 ± 2.12% for CUR and 96.11 ± 2.88% for QUE. The AOR for fresh SD-S-SNEDDS was 17.19 ± 3.11 θ and for aged SD-S-SNEDDS it was 18.32 ± 1.21 θ. A negligible difference was found between aged and fresh SD-S-SNEDDS in the values of mean DPS, percentage drug loading and AOR. Similarly a non-significant difference ($P > 0.05$) was observed in the dissolution profiles of fresh and aged SD-S-SNEDDS. More than 90% release of CUR and QUE was observed in first 5 min from fresh and aged SD-S-SNEDDS (Fig. 7C). The f2 value was found to be 74.81 for aged and fresh CUR SD-S-SNEDDS and 70.15 for aged and fresh QUE SD-S-SNEDDS powder which showed comparable dissolution profiles [70].

3.6.2. Cell line toxicity study

The results of cell line study revealed that more than 85% cells were found viable in all cases at all three concentrations i.e., 25, 12.5 and 6.25 µg/mL. The percentage cell viability at 25 µg/mL concentration for raw CUR, raw QUE, raw CUR-QUE mixture, CUR-QUE SD-S-SNEDDS powder, was found to be 88.56 ± 3.54%, 92.88 ± 3.11%, 87.21 ± 2.76% and 90.00 ± 3.12% respectively. Overall, the study indicated that the formulation was safe and did not cause any cellular toxicity as more than 90% cells were found viable [71,72].

Furthermore, in case of placebo more than 98% cells were found to viable at all concentrations indicating towards the safety of all the excipients used for formulation of SD-S-SNEDDS powder. The results are

shown in Fig. 8. For oral delivery of drugs, Caco2 cell line is the most preferred cell lines because it represents human colon/intestinal picture and absence of any toxicity due to the formulation on the cells indicate that the developed formulation is biocompatible and not going to cause any gastrointestinal toxicity [73–75].

4. Conclusion

In the present study an attempt has been made to explore the use of synbiotics containing GLEP and probiotics as solid carriers for adsorbing liquid isotropic mixture of SNEDDS. Spray drying of developed S-SNEDDS powder has further improved the micromeritic behavior of formulation along with enhanced dissolution profile and permeability of CUR and QUE. The non-significant difference in mean DPS, drug loading, AOR and dissolution profiles of fresh and aged formulations that were kept for accelerated stability studies indicated the potential synbiotics to be used as solid carriers for adsorbing L-SNEDDS. Thus this study also opened a scope for using this synbiotic composition for solidification of other lipid based delivery systems.

CRediT authorship contribution statement

Rubiya Khursheed: Methodology, Data curation, Writing – original draft. **Sachin Kumar Singh:** Conceptualization, Validation, Supervision, Writing – review & editing. **Sheetu Wadhwa:** Supervision. **Monica Gulati:** Supervision, Writing – review & editing. **Bhupinder Kapoor:** Methodology. **Subheet Kumar Jain:** Methodology. **Kuppusamy Gowthamarajan:** Methodology. **Flavia Zacconi:** Writing – review & editing. **Dinesh Kumar Chellappan:** Methodology. **Gaurav Gupta:** Methodology. **Niraj Kumar Jha:** Writing – review & editing. **Piyush Kumar Gupta:** Writing – review & editing. **Kamal Dua:** Writing – review & editing.

Acknowledgements

The work has received grant from Department of Science and Technology- fund for improvement of science and technology infrastructure in Universities and Higher Educational Institutions (DST- FIST, Grant No. SR/FST/LS-1/2017/22(C)), New Delhi.

Declaration of competing interest

Declared none.

References

[1] W. Fan, W. Zhu, X. Zhang, L. Di, The preparation of curcumin sustained-release solid dispersion by hot melt extrusion—I. Optimization of the formulation, J. Pharm. Sci. 109 (2020) 1242–1252.
[2] K. Wang, T. Zhang, L. Liu, X. Wang, P. Wu, Z. Chen, C. Ni, J. Zhang, F. Hu, J. Huang, Novel micelle formulation of curcumin for enhancing antitumor activity and inhibiting colorectal cancer stem cells, Int. J. Nanomedicine 7 (2012) 4487–4497.
[3] C. Righeschi, M.C. Bergonzi, B. Isacchi, C. Bazzicalupi, P. Gratteri, A.R. Bilia, Enhanced curcumin permeability by SLN formulation: the PAMPA approach, LWT 66 (2016) 475–483.
[4] M. Karimi, F. Gheybi, P. Zamani, M. Mashreghi, S. Golmohammadzadeh, S. A. Darban, A. Badiee, M.R. Jaafari, Preparation and characterization of stable nanoliposomal formulations of curcumin with high loading efficacy: in vitro and in vivo anti-tumor study, Int. J. Pharm. 580 (2020), 119211.
[5] R. Javani, F.S. Hashemi, B. Ghanbarzadeh, H. Hamishehkar, Quercetin-loaded niosomal nanoparticles prepared by the thin-layer hydration method: formulation development, colloidal stability, and structural properties, LWT 141 (2021), 110865.
[6] F. Sheng, P.S. Chow, J. Hu, S. Cheng, L. Guo, Y. Dong, Preparation of quercetin nanorod/microcrystalline cellulose formulation via fluid bed coating crystallization for dissolution enhancement, Int. J. Pharm. 576 (2020), 118983.
[7] M. Imran, M.K. Iqubal, K. Imtiyaz, S. Saleem, S. Mittal, M.M.A. Rizvi, J. Ali, S. Baboota, Topical nanostructured lipid carrier gel of quercetin and resveratrol: formulation, optimization, in vitro and ex vivo study for the treatment of skin cancer, Int. J. Pharm. 587 (2020), 119705.
[8] R.P. Joshi, G. Negi, A. Kumar, Y.B. Pawar, B. Munjal, A.K. Bansal, S.S. Sharma, SNEDDS curcumin formulation leads to enhanced protection from pain and functional deficits associated with diabetic neuropathy: an insight into its mechanism for neuroprotection, Nanomedicine 9 (2013) 776–785.
[9] R. Khursheed, S.K. Singh, S. Wadhwa, M. Gulati, A. Awasthi, R. Kumar, A. K. Ramanunny, B. Kapoor, P. Kumar, L. Corrie, Exploring role of probiotics and ganoderma lucidum extract powder as solid carriers to solidify liquid self-nanoemulsifying delivery systems loaded with curcumin, Carbohydr. Polym. 250 (2020), 116996.
[10] J.H. Kang, D.H. Oh, Y.-K. Oh, C.S. Yong, H.-G. Choi, Effects of solid carriers on the crystalline properties, dissolution and bioavailability of flurbiprofen in solid self-nanoemulsifying drug delivery system (solid SNEDDS), Eur. J. Pharm. Biopharm. 80 (2012) 289–297.
[11] B. Tang, G. Cheng, J.-C. Gu, C.-H. Xu, Development of solid self-emulsifying drug delivery systems: preparation techniques and dosage forms, Drug Discov. Today 13 (13–14) (2008) 606–612.
[12] P. Kaur, S.K. Singh, V. Garg, M. Gulati, Y. Vaidya, Optimization of spray drying process for formulation of solid dispersion containing polypeptide-k powder through quality by design approach, Powder Technol. 284 (2015) 1–11.
[13] S. Beg, S. Swain, H.P. Singh, C.N. Patra, M.E.B. Rao, Development, optimization, and characterization of solid self-nanoemulsifying drug delivery systems of valsartan using porous carriers, AAPS PharmSciTech 13 (2012) 1416–1427.
[14] A. Patel, P. Shelat, A. Lalwani, Development and optimization of solid self-nanoemulsifying drug delivery system (S-SNEDDS) using Scheffe's design for improvement of oral bioavailability of nelfinavir mesylate, Drug Deliv. Transl. Res. 4 (2014) 171–186.
[15] H.D. Williams, M.V. Speybroeck, P. Augustijns, C.J.H. Porter, Lipid-based formulations solidified via adsorption onto the mesoporous carrier Neusilin® US2: effect of drug type and formulation composition on in vitro pharmaceutical performance, J. Pharm. Sci. 103 (2014) 1734–1746.
[16] C. Sander, P. Holm, Porous magnesium aluminometasilicate tablets as carrier of a cyclosporine self-emulsifying formulation, AAPS PharmSciTech 10 (2009) 1388–1395.
[17] M. Van Speybroeck, H.D. Williams, T.-H. Nguyen, M.U. Anby, C.J.H. Porter, P. Augustijns, Incomplete desorption of liquid excipients reduces the in vitro and in vivo performance of self-emulsifying drug delivery systems solidified by adsorption onto an inorganic mesoporous carrier, Mol. Pharm. 9 (2012) 2750–2760.
[18] M. Milovic, J. Djuriš, L. Djekic, D. Vasiljevic, S. Ibric, Characterization and evaluation of solid self-microemulsifying drug delivery systems with porous carriers as systems for improved carbamazepine release, Int. J. Pharm. 436 (2012) 58–65.
[19] S. Beg, O.P. Katare, S. Saini, B. Garg, R.K. Khurana, B. Singh, Solid self-nanoemulsifying systems of olmesartan medoxomil: formulation development, micromeritic characterization, in vitro and in vivo evaluation, Powder Technol. 294 (2016) 93–104.
[20] R. Khursheed, S.K. Singh, S. Wadhwa, M. Gulati, A. Awasthi, Therapeutic potential of mushrooms in diabetes mellitus: role of polysaccharides, Int. J. Biol. Macromol. 164 (2020) 1194–1205.
[21] Z. Asemi, Z. Zare, H. Shakeri, S.-S. Sabihi, A. Esmaillzadeh, Effect of multispecies probiotic supplements on metabolic profiles, hs-CRP, and oxidative stress in patients with type 2 diabetes, Ann. Nutr. Metab. 63 (2013) 1–9.
[22] S. Huang, J. Mao, K. Ding, Y. Zhou, X. Zeng, W. Yang, P. Wang, C. Zhao, J. Yao, P. Xia, Polysaccharides from ganoderma lucidum promote cognitive function and neural progenitor proliferation in mouse model of Alzheimer's disease, Stem Cell Rep. 8 (2017) 84–94.
[23] L. Agerholm-Larsen, A. Raben, N. Haulrik, A. Hansen, M. Manders, A. Astrup, Effect of 8 week intake of probiotic milk products on risk factors for cardiovascular diseases, Eur. J. Clin. Nutr. 54 (2000) 288–297.
[24] K.K. Sharma, S. Chandra, D.K. Basu, Synthesis and antiarthritic study of a new orally active diferuloyl methane (curcumin) gold complex, Inorganica Chim. Acta 135 (1) (1987) 47–48.
[25] R. Srivastava, M. Dikshit, R.C. Srimal, B.N. Dhawan, Anti-thrombotic effect of curcumin, Thromb. Res. 40 (1985) 413–417.
[26] M. Kaur, A. Singh, B. Kumar, S.K. Singh, A. Bhatia, M. Gulati, T. Prakash, P. Bawa, A.H. Malik, Protective effect of co-administration of curcumin and sildenafil in alcohol induced neuropathy in rats, Eur. J. Pharmacol. 805 (2017) 58–66.
[27] R. Shafabakhsh, M. Mobini, F. Raygan, E. Aghadavod, V. Ostadmohammadi, E. Amirani, M.A. Mansournia, Z. Asemi, Curcumin administration and the effects on psychological status and markers of inflammation and oxidative damage in patients with type 2 diabetes and coronary heart disease, Clin. Nutr. ESPEN 40 (2020) 77–82.
[28] E.M. Abdelsamia, S.A. Khaleel, A. Balah, N.A. Abdel Baky, Curcumin augments the cardioprotective effect of metformin in an experimental model of type I diabetes mellitus; impact of Nrf2/HO-1 and JAK/STAT pathways, Biomed. Pharmacother. 109 (2019) 2136–2144.
[29] S. Patra, B. Pradhan, R. Nayak, C. Behera, L. Rout, M. Jena, T. Efferth, S.K. Bhutia, Chemotherapeutic efficacy of curcumin and resveratrol against cancer: chemoprevention, chemoprotection, drug synergism and clinical pharmacokinetics, Semin. Cancer Biol. 73 (2021) 310–320, https://doi.org/10.1016/j.semcancer.2020.10.010.
[30] Z. Dehghani, A.A. Meratan, A.A. Saboury, M. Nemat-Gorgani, a-synuclein fibrillation products trigger the release of hexokinase I from mitochondria: protection by curcumin, and possible role in pathogenesis of Parkinson's disease, Biochim. Biophys. Acta Biomembr. 1862 (2020), 183251.

[31] M.H. Castillo, E. Perkins, J.H. Campbell, R. Doerr, J.M. Hassett, C. Kandaswami, E. Middleton, The effects of the bioflavonoid quercetin on squamous cell carcinoma of head and neck origin, Am. J. Surg. 158 (1989) 351–355.
[32] V. Jaishree, S. Narsimha, Swertiamarin and quercetin combination ameliorates hyperglycemia, hyperlipidemia and oxidative stress in streptozotocin-induced type 2 diabetes mellitus in wistar rats, Biomed. Pharmacother. 130 (2020), 110561.
[33] Y. Hu, Z. Gui, Y. Zhou, L. Xia, K. Lin, Y. Xu, Quercetin alleviates rat osteoarthritis by inhibiting inflammation and apoptosis of chondrocytes, modulating synovial macrophages polarization to M2 macrophages, Free Radic. Biol. Med. 145 (2019) 146–160.
[34] J. Lu, Y. Meng, R. Wang, R. Zhang, Anti-arrhythmogenic effects of quercetin postconditioning in myocardial ischemia/reperfusion injury in a rat model, J. King Saud Univ. Sci. 32 (2020) 1910–1916.
[35] J. Jyoti, N.K. Anandhakrishnan, S.K. Singh, B. Kumar, M. Gulati, K. Gowthamarajan, R. Kumar, A.K. Yadav, B. Kapoor, N.K. Pandey, S. Som, S. Mohanta, I. Melkani, R. Khursheed, R. Narang, A three-pronged formulation approach to improve oral bioavailability and therapeutic efficacy of two lipophilic drugs with gastric lability, Drug Deliv. Transl. Res. 9 (2019) 848–865.
[36] M. Lu, H. Xing, J. Jiang, X. Chen, T. Yang, D. Wang, P. Ding, Liquisolid technique and its applications in pharmaceutics, Asian J. Pharm. Sci. 12 (2017) 115–123.
[37] S.K. Singh, K.K. Srinivasan, K. Gowthamarajan, D. Prakash, N.B. Gaikwad, D. S. Singare, Influence of formulation parameters on dissolution rate enhancement of glyburide using liquisolid technique, Drug Dev. Ind. Pharm. 38 (2012) 961–970.
[38] B. Kumar, V. Garg, S. Singh, N.K. Pandey, A. Bhatia, T. Prakash, M. Gulati, S. K. Singh, Impact of spray drying over conventional surface adsorption technique for improvement in micromeritic and biopharmaceutical characteristics of self-nanoemulsifying powder loaded with two lipophilic as well as gastrointestinal labile drugs, Powder Technol. 326 (2018) 425–442.
[39] D.S. Singare, S. Marella, K. Gowthamrajan, G.T. Kulkarni, R. Vooturi, P.S. Rao, Optimization of formulation and process variable of nanosuspension: an industrial perspective, Int. J. Pharm. 402 (2010) 213–220.
[40] F. Kesisoglou, S. Panmai, Y. Wu, Nanosizing–oral formulation development and biopharmaceutical evaluation, Adv. Drug Deliv. Rev. 59 (2007) 631–644.
[41] S. Mohanta, S.K. Singh, B. Kumar, M. Gulati, J. Jyoti, S. Som, S. Panchal, I. Melkani, M. Banerjee, S.K. Sinha, Solidification of liquid modified apple polysaccharide by its adsorption on solid porous carriers through spray drying and evaluation of its potential as binding agent for tablets, Int. J. Biol. Macromol. 120 (2018) 1975–1998.
[42] S. Mohanta, S.K. Singh, B. Kumar, M. Gulati, J. Jyoti, S. Som, S. Panchal, I. Melkani, M. Banerjee, S.K. Sinha, R. Khursheed, A.K. Yadav, V. Verma, R. Kumar, D.S. Sharma, A.H. Malik, N.K. Pandey, S. Wadhwa, Solidification of liquid Modified Apple Polysaccharide by its adsorption on solid porous carriers through spray drying and evaluation of its potential as binding agent for tablets, Int. J. Biol. Macromol. 120 (2018) 1975–1998.
[43] P. Sharma, S.K. Singh, N.K. Pandey, S.Y. Rajesh, P. Bawa, B. Kumar, M. Gulati, S. Singh, S. Verma, A.K. Yadav, S. Wadhwa, S.K. Jain, K. Gowthamarajan, A. H. Malik, S. Gupta, R. Khursheed, Impact of solid carriers and spray drying on pre/post-compression properties, dissolution rate and bioavailability of solid self-nanoemulsifying drug delivery system loaded with simvastatin, Powder Technol. 338 (2018) 836–846.
[44] R. Kumar, R. Khursheed, R. Kumar, A. Awasthi, N. Sharma, S. Khurana, B. Kapoor, N. Khurana, S.K. Singh, K. Gowthamarajan, Self-nanoemulsifying drug delivery system of fisetin: formulation, optimization, characterization and cytotoxicity assessment, J. Drug Delivery Sci. Technol. 54 (2019), 101252.
[45] S.K. Singh, K.K. Srinivasan, K. Gowthamarajan, D. Prakash, N.B. Gaikwad, D. S. Singare, Influence of formulation parameters on dissolution rate enhancement of glyburide using liquisolid technique, Drug Dev. Ind. Pharm. 38 (2012) 961–970.
[46] Varun, Puneet, K. Sachin Singh, Bimlesh, Palak, Monica, K. Ankit Yadav, Solid self-nanoemulsifying drug delivery systems for oral delivery of polypeptide-k: Formulation, optimization, in-vitro and in-vivo antidiabetic evaluation, Eur. J. Pharm. Sci. 109 (2017) 297–315.
[47] N. Malanovic, K. Lohner, Gram-positive bacterial cell envelopes: the impact on the activity of antimicrobial peptides, Biochim. Biophys. Acta Biomembr. 1858 (2016) 936–946.
[48] T.J. Silhavy, D. Kahne, S. Walker, The bacterial cell envelope, Cold Spring Harb. Perspect. Biol. 2 (2010) a000414–a00041<label/>4.
[49] G. Kaur, S.K. Singh, R. Kumar, B. Kumar, Y. Kumari, M. Gulati, N.K. Pandey, K. Gowthamarajan, D. Ghosh, A. Clarisse, S. Wadhwa, M. Mehta, S. Satija, K. Dua, H. Dureja, S. Gupta, P.K. Singh, B. Kapoor, N. Chitranshi, A. Kumar, O. Porwal, Development of modified apple polysaccharide capped silver nanoparticles loaded with mesalamine for effective treatment of ulcerative colitis, J. Drug Deliv. Sci. Technol. 60 (2020), 101980.
[50] M. Danaei, M. Dehghankhold, S. Ataei, F. Hasanzadeh Davarani, R. Javanmard, A. Dokhani, S. Khorasani, M.R. Mozafari, Impact of particle size and polydispersity index on the clinical applications of lipidic nanocarrier systems, Pharmaceutics 10 (2) (2018).
[51] M. Instruments, Dynamic light scattering common terms defined, in: Inform White Paper.[Google Scholar], 2011.
[52] B. Choudhary, S.R. Paul, S.K. Nayak, V.K. Singh, A. Anis, K. Pal, Understanding the effect of functionalized carbon nanotubes on the properties of tamarind gum hydrogels, Polym. Bull. 75 (2018) 4929–4945.
[53] K. Nakaya, H. Ushio, S. Matsukawa, M. Shimizu, T. Ohshima, Effects of droplet size on the oxidative stability of oil-in-water emulsions, Lipids 40 (5) (2005) 501–507.
[54] J. Jiang, G. Oberdörster, P. Biswas, Characterization of size, surface charge, and agglomeration state of nanoparticle dispersions for toxicological studies, J. Nanopart. Res. 11 (2009) 77–89.
[55] S. Verma, R. Gokhale, D.J. Burgess, A comparative study of top-down and bottom-up approaches for the preparation of micro/nanosuspensions, Int. J. Pharm. 380 (1–2) (2009) 216–222.
[56] R.H. Müller, C. Jacobs, O. Kayser, Nanosuspensions as particulate drug formulations in therapy. rationale for development and what we can expect for the future, Adv. Drug Deliv. Rev. 47 (1) (2001) 3–19.
[57] S.K. Singh, Y. Vaidya, M. Gulati, S. Bhattacharya, V. Garg, N.K. Pandey, Nanosuspension: principles, perspectives and practices, Curr. Drug Deliv. 13 (8) (2016) 1222–1246.
[58] K.V. Mahesh, S.K. Singh, M. Gulati, A comparative study of top-down and bottom-up approaches for the preparation of nanosuspensions of glipizide, Powder Technol. 256 (2014) 436–449.
[59] R.P. Joshi, G. Negi, A. Kumar, Y.B. Pawar, B. Munjal, A.K. Bansal, S.S. Sharma, SNEDDS curcumin formulation leads to enhanced protection from pain and functional deficits associated with diabetic neuropathy: an insight into its mechanism for neuroprotection, Nanomedicine 9 (6) (2013) 776–785.
[60] M. Kazi, A.A. Shahba, S. Alrashoud, M. Alwadei, A.Y. Sherif, F.K. Alanazi, Bioactive self-nanoemulsifying drug delivery systems (Bio-SNEDDS) for combined oral delivery of curcumin and piperine, Molecules 25 (7) (2020).
[61] M. Shukla, S. Jaiswal, A. Sharma, P.K. Srivastava, A. Arya, A.K. Dwivedi, J. Lal, A combination of complexation and self-nanoemulsifying drug delivery system for enhancing oral bioavailability and anticancer efficacy of curcumin, Drug Dev. Ind. Pharm. 43 (5) (2017) 847–861.
[62] T.H. Tran, Y. Guo, D. Song, R.S. Bruno, X. Lu, Quercetin-containing self-nanoemulsifying drug delivery system for improving oral bioavailability, J. Pharm. Sci. 103 (3) (2014) 840–852.
[63] N. Ahmad, R. Ahmad, A.A. Naqvi, M.A. Alam, R. Abdur Rub, F.J. Ahmad, Enhancement of quercetin oral bioavailability by self-nanoemulsifying drug delivery system and their quantification through ultra high performance liquid chromatography and mass spectrometry in cerebral ischemia, Drug Res. (Stuttg.) 67 (10) (2017) 564–575.
[64] O.A.A. Ahmed, S.M. Badr-Eldin, M.K. Tawfik, T.A. Ahmed, K.M. El-Say, J.M. Badr, Design and optimization of self-nanoemulsifying delivery system to enhance quercetin hepatoprotective activity in paracetamol-induced hepatotoxicity, J. Pharm. Sci. 103 (2) (2014) 602–612.
[65] P. Arya, N. Raghav, In-vitro studies of curcumin-ß-cyclodextrin inclusion complex as sustained release system, J. Mol. Struct. 1228 (2021), 129774.
[66] T. Pralhad, K. Rajendrakumar, Study of freeze-dried quercetin–cyclodextrin binary systems by DSC, FT-IR, X-ray diffraction and SEM analysis, J. Pharm. Biomed. Anal. 34 (2) (2004) 333–339.
[67] D.A. Bhagwat, P.A. Swami, S.J. Nadaf, P.B. Choudhari, V.M. Kumbar, H.N. More, S. G. Killedar, P.S. Kawtikwar, Capsaicin loaded solid SNEDDS for enhanced bioavailability and anticancer activity: in-vitro, in-silico, and in-vivo characterization, J. Pharm. Sci. 110 (1) (2021) 280–291.
[68] N. Zhang, F. Zhang, S. Xu, K. Yun, W. Wu, W. Pan, Formulation and evaluation of luteolin supersaturatable self-nanoemulsifying drug delivery system (S-SNEDDS) for enhanced oral bioavailability, J. Drug. Deliv. Sci. Technol. 58 (2020), 101783.
[69] T. Kanwal, M. Kawish, R. Maharjan, I. Ghaffar, H.S. Ali, M. Imran, S. Perveen, S. Saifullah, S.U. Simjee, M.R. Shah, Design and development of permeation enhancer containing self-nanoemulsifying drug delivery system (SNEDDS) for ceftriaxone sodium improved oral pharmacokinetics, J. Mol. Liq. 289 (2019), 111098.
[70] V.P. Shah, Y. Tsong, P. Sathe, J.P. Liu, In vitro dissolution profile comparison–statistics and analysis of the similarity factor, f2, Pharm. Res. 15 (6) (1998) 889–896.
[71] S.Y. Rajesh, S.K. Singh, N.K. Pandey, P. Sharma, P. Bawa, B. Kumar, M. Gulati, S. K. Jain, K. Gowthamarajan, S. Singh, Impact of various solid carriers and spray drying on pre/post compression properties of solid SNEDDS loaded with glimepiride: in vitro-ex vivo evaluation and cytotoxicity assessment, Drug Dev. Ind. Pharm. 44 (7) (2018) 1056–1069.
[72] R. Kumar, R. Khursheed, R. Kumar, A. Awasthi, N. Sharma, S. Khurana, B. Kapoor, N. Khurana, S.K. Singh, K. Gowthamarajan, A. Wadhwani, Self-nanoemulsifying drug delivery system of fisetin: Formulation, optimization, characterization and cytotoxicity assessment, J. Drug Deliv. Sci. Technol. 54 (2019), 101252.
[73] Y. Sambuy, I. De Angelis, G. Ranaldi, M.L. Scarino, A. Stammati, F. Zucco, The Caco-2 cell line as a model of the intestinal barrier: influence of cell and culture-related factors on Caco-2 cell functional characteristics, Cell Biol. Toxicol. 21 (1) (2005) 1–26.
[74] A.G.F. Boim, J. Wragg, S.G. Canniatti-Brazaca, L.R.F. Alleoni, Human intestinal Caco-2 cell line in vitro assay to evaluate the absorption of cd, cu, mn and zn from urban environmental matrices, Environ. Geochem. Health 42 (2) (2020) 601–615.
[75] E. Róka, Z. Ujhelyi, M. Deli, A. Bocsik, É. Fenyvesi, L. Szente, F. Fenyvesi, M. Vecsernyés, J. Váradi, P. Fehér, R. Gesztelyi, C. Félix, F. Perret, I.K. Bácskay, Evaluation of the cytotoxicity of a-cyclodextrin derivatives on the Caco-2 cell line and human erythrocytes, Molecules 20 (11) (2015) 20269–20285.